Universidade de Aveiro
Ano 2012

Departamento de Engenharia de Materiais e Cerâmica

MARIANA DA SILVA MARINHO

BIOCOMPATIBLE POLYMERIC COATINGS FOR BONE TISSUE REGENERATION

Universidade de Aveiro
Ano 2012
Departamento de Engenharia de Materiais e Cerâmica

MARIANA DA SILVA MARINHO

BIOCOMPATIBLE POLYMERIC COATINGS FOR BONE TISSUE REGENERATION

Dissertação apresentada à Universidade de Aveiro para cumprimento dos requisitos necessários à obtenção do grau de Mestre em Materiais e Dispositivos Biomédicos, realizada sob a orientação científica da Dra. Helena Fernandes e da Dra. Paula Vilarinho, ambas Professoras associadas do Departamento de Engenharia de Materiais e Cerâmica da Universidade de Aveiro.

o júri

presidente

Prof. Doutor Rui Ramos Ferreira e Silva
Professor Associado da Universidade de Aveiro

Doutora Ana Luísa Daniel da Silva
Equiparada a Investigadora Auxiliar da Universidade de Aveiro

Prof. Doutora Maria Helena Figueira Vaz Fernandes
Professora Associada da Universidade de Aveiro

Prof. Doutora Paula Maria Lousada Silveirinha Vilarinho
Professora Associada da Universidade de Aveiro

agradecimentos

Em primeiro lugar gostaria de expressar a minha gratidão às minhas orientadoras Dra. Helena Fernandes e Dra. Paula Vilarinho pelo apoio prestado, pela orientação, pelo conhecimento partilhado e particularmente pela oportunidade.
Em segundo lugar obviamente agradeço à Nathalie Barroca, pela sua constante assistência e disponibilidade, pela força transmitida e pela amizade. A sua ajuda foi indiscutivelmente valiosa no desenvolvimento deste trabalho, e daí toda a minha gratidão e admiração.
Agradeço também a todos os técnicos do departamento e alunos de doutoramento que de alguma forma estiveram envolvidos no trabalho e que se dispuseram a ajudar, principalmente nas alturas de maior urgência.
Aos colegas de laboratório pela companhia, pelas dicas e pelas conversas e brincadeiras.
Aos meus amigos, tanto aos que me desejam sucesso mesmo estando distantes, como aos que estiveram mais presentes e me acompanharam durante todo este processo.
Aos meus familiares, com um especial e enorme agradecimento aos meus pais por me terem proporcionado a oportunidade de alcançar esta etapa e pelo apoio nos desabafos, e ao meu irmão Zé Pedro, pelo exemplo de pessoa que é, e pela força e confiança que me transmite.

No fundo, um sincero “muito obrigada!” a toda e qualquer pessoa que acreditou em mim e nas minhas capacidades, mesmo quando eu duvidei. Desejo-lhes o melhor.

palavras-chave Ácido poli(L-láctico), aço, adesão, teste fita-cola, spin-coating.

resumo

Um dos grandes desafios da investigação biomédica é ultrapassar as taxas de rejeição de próteses implantadas melhorando as suas propriedades como biomateriais, garantindo assim maior qualidade de vida aos pacientes. Grande parte destas próteses é constituída por componentes metálicas que, por serem inertes, surge uma necessidade de as melhorar. Uma das soluções reside no revestimento do metal por um polímero, de preferência com capacidade de induzir a regeneração óssea.

Neste trabalho testou-se a adesão entre o aço 316L, material muito utilizado como biomaterial, e o ácido poli(L-láctico) (PLLA), um polímero, biocompatível, de biodegradação controlável, bioabsorvível, piezoeléctrico e aprovado pela Food and Drug Administration (FDA). O filme de PLLA foi depositado no aço por spin-coating e procedeu-se à investigação do efeito de diferentes variáveis na adesão, nomeadamente tratamento físico de superfície (por polimento), tratamento químico de superfície (por silanização), peso molecular do PLLA, cristalinidade do filme, espessura, e imersão numa solução tampão de fosfatos (PBS).

A adesão entre os dois materiais foi estudada utilizando um teste qualitativo, o teste da fita-cola, seguindo a norma ASTM D3359. Observou-se que os filmes preparados da solução de PLLA de menor peso molecular apresentaram os melhores resultados no teste da fita-cola, principalmente quando depositada nas amostras de aço com maior rugosidade. O efeito da espessura do filme, foi testado com diferentes concentrações da solução de PLLA de menor peso molecular, concluindo-se que quanto menor a concentração da solução de polímero, menor a espessura do filme e melhor a sua adesão ao substrato. Por conseguinte, estas condições de polimento (P180 e P400) foram selecionadas para prosseguirem para caracterização adicional: cristalização e posterior ensaio de degradação em fluido sintético (PBS), com a duração de uma semana, um mês e dois meses. Os resultados apontam para uma significativa perda de adesão, uma vez que a adesão do filme ao substrato resultou enfraquecida após a imersão.

Ensaios preliminares de silanização dos substratos de aço não revelaram melhorias significativas da adesão dos filmes ao substrato comparativamente aos obtidos por tratamento físico da superfície.

Em conclusão, os resultados deste trabalho mostram que é possível produzir revestimentos de PLLA sobre aço 316L e controlar a adesão do filme de PLLA ao substrato de aço através de tratamentos de superfície e de variações nas características do filme. Assim a combinação destes dois materiais parece ser adequada para potenciais aplicações biomédicas.

keywords PLLA, stainless steel, adhesion, tape test, spin-coating.

abstract

One of the major challenges in biomedical research is to overcome the rejection rates of implanted prostheses improving their properties as biomaterials, thus ensuring greater quality of life for the patients. Many of this prosthesis include inert metallic components, hence the necessity of improvement. One of the solutions lies in the polymeric coating, preferably one with the ability to induce bone regeneration.

In this study we tested the adhesion between the 316L stainless steel, a material widely used as a biomaterial, and poly (L-lactic acid) (PLLA), a polymer, biocompatible, with controlled biodegradation, bioabsorbable, piezoelectric and approved by the Food and Drug Administration (FDA). The PLLA film was deposited onto the stainless steel samples by spin-coating and proceeded to the investigation of the effect of different variables in the adhesion, namely substrate surface physical treatment (by grinding), substrate surface chemical treatment (by silanization), PLLA molecular weight, film crystallinity, film thickness and immersion into *phosphate buffered saline* (PBS) solution.

The adhesion between both materials was studied using a qualitative test, the tape test, following a standard (ASTM D3359). It was observed that films prepared with the lower molecular weight PLLA solution presented the best results in the tape test, especially when deposited onto the substrates with higher roughness. The effect of film thickness was tested with different solution concentrations of the lower molecular weight PLLA solution, concluding that the lower the solution concentration, the thinner the film and the better the adhesion of the film to the substrate. Therefore, these polishing conditions (P180 and P400) were chosen for further characterization: crystallization and subsequent degradation assay in a synthetic fluid (PBS) for one week, one month and two months. These results point at a significant loss of adhesion, since the adhesion of the film to the substrate after immersion resulted weakened.

Preliminary tests of silanization of steel substrates showed no significant improvements in the film adhesion to the substrate, when compared to the results already obtained only with a surface physical treatment.

In conclusion, the results obtained during this work show that it is possible to produce PLLA coatings on 316L stainless steel substrates and to control the adhesion of PLLA films to substrate through surface treatments and variations in the film characteristics. Therefore, the combination of these materials appears to be potentially suitable for biomedical applications.

Table of Contents

List of Figures

List of Tables

List of Abbreviations

AFM	Atomic Force Microscopy
APTES	3-(aminopropyl)triethoxysilane
ASTM	American Society for Testing and Materials
BCC	Body Centered Cubic
DSC	Differential Scanning Calorimetry
EDS	Energy Dispersive X-ray Spectroscopy
FCC	Face Centered Cubic
FDA	Food and Drug Administration
HIV	Human Immunodeficiency Virus
ISO	International Organization for Standardization
PBS	Phosphate Buffered Saline
PDLA	Poly-D-lactic acid
PEG	Poly(ethylene glycol)
PLA	Poly (lactic acid)
PLLA	Poly-L-lactic acid
SEM	Scanning Electron Microscopy
XRD	X-Ray Diffraction

Chapter 1 - INTRODUCTION

1.1 Motivation and Objectives

Metallic materials, such as stainless steels and cobalt-chromium alloys, have been used as orthopedic implants since some decades. Despite all of the advantages they present, these materials may experience some problems such as deslocation or bone resorption, which is the loss of bone substance. As an example, in total hip replacement, prosthesis loosening can occur due to bone resorption in the proximal femur, caused by the stress in the femoral cortex after metal implementation [1]. Mainly for this reason, it is estimated that between 10% and 20% of joint implant need to be replaced within 15 to 20 years [2]. In order to overcome these limitations and minimize rejections, the metal coating with a material that can stimulate integration or even bone regeneration appears as a quite interesting solution. Within this context the use of a piezoelectric biopolymer arises as a hypothesis that should be explored. Because of the disadvantages presented by metallic and ceramic biomaterials, polymers have been gradually introduced in clinical use, presenting great advantages as easy shaping and their low cost, as well as superior physical properties. Biodegradable polymers such as polyesters (polylactic acid and polyglycolic acid) have been receiving major attention for their use in tissue engineering. Moreover, it is known that the electrical activity of a surface can enhance protein adhesion and cellular development, all of which are essential in tissue regeneration, particularly at the bone-implant interface. It is precisely why poly-L-lactic acid (PLLA), a form of polylactic acid (PLA), is of particular interest as a possible coating for metallic prostheses parts since it is piezoelectric (i.e. having the ability to generate an electric charge by action of a mechanical deformation and vice versa). This peculiarity associated with other characteristics such as biodegradability, biocompatibility and bioabsorbability, in addition to the fact that it is a FDA (Food and Drug Administration) approved material for sutures lines and screws (among others) justifies the exploitation of PLLA coated metals to promote bone regeneration process and decrease the prostheses acceptance time and rejection rate.

Based on these assumptions and evidences this work exploits the adhesion of PLLA films to 316L stainless steel (widely used in hip prostheses), in order to optimize the adhesion of the polymeric film to the substrate for biomedical applications.

The main goals of this work comprise the study of the effects of:

i) polymer molecular weight,
ii) film thickness,
iii) substrate roughness,
iv) crystallization and
v) silanization.

It is expected to establish guide lines concerning the most suitable treatment to the metal surface and some of the optimal characteristics of the polymeric film, for adhesion optimization, in order to continue these studies for further investigation, as for example, *in vivo* studies.

1.2 Literature Review

Tissue engineering has become one of the leading areas in the academic and industrial world in the past three decades [3]. It is defined as a multidisciplinary field based in biological, chemical and engineering principles, aiming at the development of artificial constructs for repairing, replacing, maintaining or improving tissue or organ function, with recourse to biomaterials, cells and growth factors [4]. A biomaterial, in turn, can be described as any material intended to interface with biological systems in order to analyze, treat, increase or replace any tissue, organ or body function [5]. The required characteristic to qualify a material as a biomaterial is biocompatibility, i.e., the ability to create an adequate tissue response in a specific application [6]. This ability is dependent on various factors such as chemical, physical and biological properties of the material, as well as on the shape and structure of the implant.

Some biomaterials also exhibit others characteristics such as bioactivity and biodegradability. Concerning the type of interaction with living tissues, a biomaterial can either be:

- inert, with none or minimal response from the host tissue; or
- bioactive, with bonding and integration by the stimulation of new tissue growth [7].

The terms biodegradability and bioresorption refer to the case when the material dissolves itself in the body with time, offering the possibility to overcome the disadvantages of residual solids which may result from abrasion or wear. Some requirements must be fulfilled by ideal biodegradable materials such as adequate initial strength, stiffness and retention of mechanical properties to assure the proper biofunctionality [8] and non-toxicity of degradation by-products [9]. Other properties must be met according to their application, as for example controlled mechanical, electrochemical and biochemical properties.

Biomaterials have been widely used in many clinical applications such as orthopedics, plastic and reconstructive surgery, cardiovascular surgery and dentistry. Some of the most common examples of these materials are breast implants, contact lenses, hip prosthesis, dental implants, vascular grafts and stents. These and other applications are represented in Figure 1.

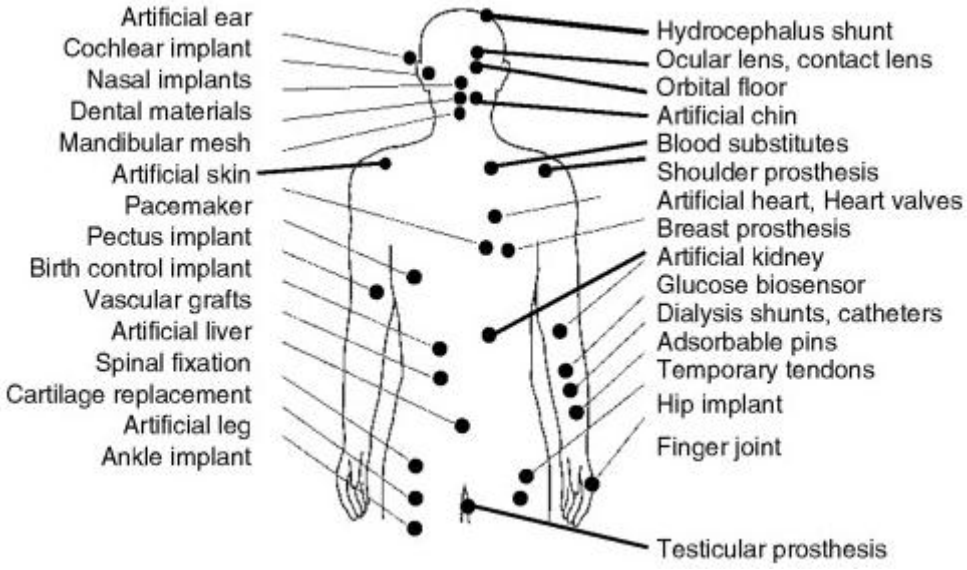

Figure 1 - Applications of biomaterials throughout the body. [10]

1.2.1 PLLA

Poly(α-hydroxyl esters), such as poly(lactic acid) (PLA), are synthetic polymers that have been extensively used in tissue engineering. PLA monomer, lactic acid (Figure 2), is a chiral molecule that exists as two optical isomers, the L and the D isomer [11], as represented on Figure 3, although sometimes it is reported a third isomer, the meso-lactide (D,L) [12]. Polymeric chains of the first two are usually referred to as PLLA and PDLA, respectively, having the same chemical and physical properties. Moreover, they are both found in bacterial systems [13], whilst PLLA is more commonly used due to the fact that its isomer, L-lactic acid, is released during the PLA hydrolysis, therefore being naturally available.

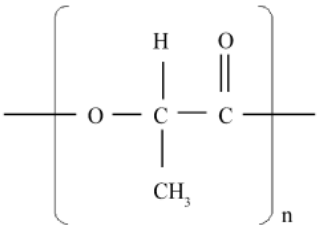

Figure 2 - Poly-lactic acid (PLA) formula. [14]

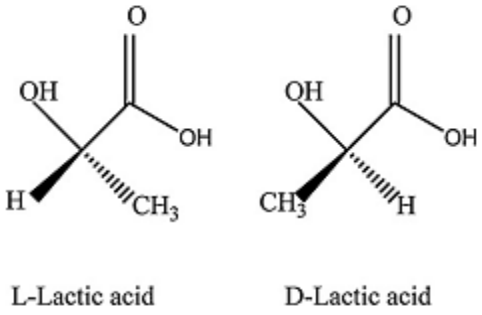

Figure 3 - Molecular structure of PLLA and PDLA, respectively. [12]

1.2.1.1. Properties

PLLA, general formula being poly-(O–CO–CH(CH3))n [15, 16], has been well documented for its excellent properties, such as biodegradability, biocompatibility and nontoxicity, and has been approved for human uses by the US Food and Drug Administration (FDA) [17-20], specifically for the correction of facial lipoatrophy in patients infected with the human immunodeficiency virus (HIV) [21]. It was the potentially controlled biodegradability characteristic, along with the mechanical stability, that made PLLA a complement to ceramic and metal implants, enabling the avoidance of a removal surgery [22]. Due to its mechanical properties (Table 1) [9], PLLA appears as a suitable material for human bone applications.

Table 1 - PLLA mechanical properties. [9]

	Young Modulus (GPa)	**Tensile strength (MPa)**	**Flexural Modulus (GPa)**	**Flexural Strength (MPa)**	**Strain Break (%)**
PLLA	3-4	50-70	4-5	100	4

PLLA is an optically active semi-crystalline polymer, with reported 37% crystallinity, even though this is dependent on the molecular weight and on the processing parameters. Pure PLLA has a melting point of 207 ºC although, due to structure

imperfections and impurities, typical PLLA melting points are between 170–180 ºC [12, 23, 24]. Its glass transition temperature is around 60-65 ºC and the water contact angle is often reported between 70º and 90º [25].

Another essential property of this polymer highlighted in literature [15, 16] is its piezoelectricity. This phenomenon, defined as the internal generation of electrical charge resulting from an applied mechanical force (direct piezoelectric effect) or the internal generation of a mechanical strain resulting from an applied electrical field (inverse piezoelectric effect), is is the consequence of the ordering of the chiral carbon atoms present in the repeating units.

1.2.1.2. Synthesis and Degradation

Lactic acid can be synthesized not only by natural but also by synthetic ways. Naturally, lactic acid is produced in mammalian muscles during glycogenolysis. It is synthesized from pyruvate in the lactic acid dehydrogenase catalyzed reaction under oxygen limiting conditions [13]. In contrast, there are different synthetic ways to prepare this material, such as polycondensation (condensation polymerization), ring-opening polymerization [24] (Figure 4), chain extension and grafting [9].

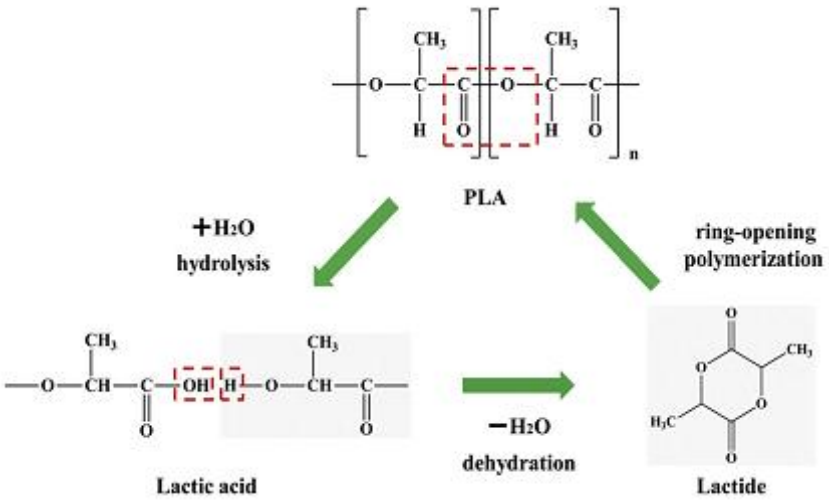

Figure 4 - Schematic illustrating of PLA hydrolysis and ring-opening polymerization. [26]

In general, all PLA forms are soluble in dioxane, acetonitrile, chloroform, methylene chloride, 1,1,2-trichloroethane and dichloroacetic acid. Crystalline PLLA, however, is not soluble in acetone, ethyl acetate or tetrahydrofuran [27].

As far as degradation is concerned, there are several factors affecting the degradation of polymers, namely the polymer characteristics (chemical structure, molecular weight and distribution, crystallinity or impurities), the fabrication processes (type of process, thermal treatment or surface topography) and the degradation conditions (solution or site of implantation) [28]. During metabolization in vivo, PLLA is degraded into lactic acid by hydrolytic de-esterification in the carboxylic acid cycle, where the monomers are expelled by the lungs as water and carbon dioxide [14-16]. Despite the degradation products being already biocompatible, this biocompatibility can be improved by controlling the degradation rate, which, in turn, can reduce the intensity of the inflammatory response [29]. Therefore it is essential to control the degradation rate, even though it can be affected by several factors, such as molecular weight, physical and chemical structure of the implant, crystallinity degree, porosity and hydrophobicity [30].

1.2.1.3. Advantages and disadvantages

As stated above, PLLA is one of the most interesting material in tissue engineering as a result of the natural degradation metabolites, easy processing into complex shapes [25] and a degradation rate that can match the healing time of damaged human tissues [17] or be tailored by proper polymer crystallization. In addition, this material is highly anisotropic and is a good piezoelectric polymer [16].

However, it should be taken into account the handicaps of the material. For instance, PLLA can cause inflammatory and allergenic reactions as a result of the hydrolytic degradation and the decrease in local pH [31]. Moreover, the released oligomers and monomers can involve a potential risk of tumor formation. This also happens because PLLA presents low cell adhesion, related to its hydrophobic surface, but many surface modification techniques can be applied to overcome such drawback. These modifications aim to introduce functional groups or molecules to create cell-biomaterial interfaces, conducting to cell attachment and spreading. Examples of such modifications include plasma treatment to increase hydrophilicity [22] and the combination of cell-adhesive

proteins such as collagen, chitosan and gelatin, proven to significantly improve the cytocompatibility [32].

1.2.1.4. Applications and state of the art

Plastic products have become viable alternatives for economic, practical and safety reasons, not only in the medical field but also in agriculture, textile, packaging and hygiene applications. Specifically in medical applications PLLA has been employed in both animals and humans since it was approved by the FDA, and an increasing amount of literature is devoted to the subject. PLLA has been widely used in many shapes, for instance fibers, films, scaffolds or pellets, due its potential applications in orthopedic and dental implants and drug delivery systems. Moreover, this polymer can also be used as a blender or a co-polymer in order to improve required properties according to the application. Some examples of PLLA based polymers used in medical fields ranges from sutures, suture anchors, screws, plates, bone pins and rods [24, 33] to drug delivery supports. In addition, this material is also well-known for its injectable form to restore or correct facial fat loss in people with the human immunodeficiency virus (HIV) [21].

Concerning PLLA films, research has been extensively done [20, 23, 29, 34-43] with different purposes and modifications, even though the predominant goals are focused either on the improvement of cell adhesion to the film or on the improvement of mechanical properties. However, for the scope of this work, PLLA is not used for neither of these reasons, as our goal is to assess PLLA adhesion to another biomaterial (316L stainless steel).

1.2.2 316L Stainless Steel

Metallic materials are inorganic substances that can be used as a pure element, although they are more often mixed with other elements to form an alloy, in order to obtain better properties than those presented by each of the elements itself. The choice of metals or alloys as biomaterials is influenced by three main factors [44]:

- biocompatibility,

- physical and mechanical properties, such as strength and toughness, and
- material degradation.

In general, metallic materials are used in many fields, from mechanics and electronics to medicine. The main medical applications for metallic materials are: internal devices, orthodontics, artificial organs and orthopedics. In fact, the majority of biomedical devices in use nowadays is made from metal alloys, and the most common include cobalt alloys, titanium and its alloys, and stainless steels.

1.2.2.1. Properties

Stainless steels are classified as bioinert materials, and are divided into three classes according to the main phase constituent of the microstructure: martensitic, ferritic or austenitic, being all of them registered in ASTM F899-95 (Standard Specification for Stainless Steel for Surgical Instruments) [45, 46].

Concerning 316L stainless steel, the required form as an implant biomaterial under ASTM specifications is single-phase austenite face centered cubic (FCC) and there should be no free ferritic body centered cubic (BCC) or carbide phases in the microstructure (Figure 5) [6]. In opposition to the martensitic and ferritic stainless steels, austenitic steels are not magnetic, being the most resistant to corrosion due to the high content of chromium and the presence of nickel in the composition [45].

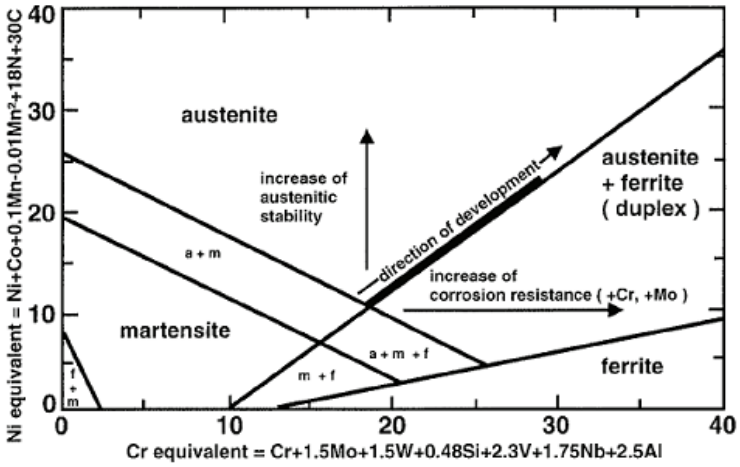

Figure 5 - Phase diagram of stainless steel. [47]

For implant use, the 316L stainless steel is the most common among the stainless steels. The chemical composition of this steel is: 60-65% iron with additions of chromium (17-20%) and nickel (12-14%), and small amounts of manganese, nitrogen, phosphorus, molybdenum, silicon and sulfur. Since this steel is significantly used as an implant metal, it is necessary to reduce the possibility of in vivo corrosion, therefore the low content of carbon (less than 0,03%). Above this amount, formation of carbides can occur, precipitating at grain boundaries and preventing the formation of a chromium-based oxide protective layer [6]. Consequently, since the surface properties determine the success or failure of the stainless steel based implant, there might be the need of surface treatment to improve corrosion resistance and biocompatibility, without affecting the physical and mechanical properties [48].

Regarding these mechanical properties, the tensile strength is within the range of 465 and 950 MPa, depending greatly on the processing, with cold worked metal much stronger than the annealed one, and the Young's modulus being around 200 GPa, apart from the type of processing [49].

1.2.2.2. Advantages and Disadvantages

Being a metallic material, 316L stainless steel present advantageous mechanical properties, including excellent ductility, good corrosion resistance, high strength under elevated temperatures, good weldability, high tensile strength and fatigue resistance, as well as low cost, ease of fabrication and good biocompatibility, thus being ideal for medical devices and suitable for load bearing applications [7, 50].

However, despite the high modulus and toughness, metallic devices are plagued with numerous deficiencies and limitations. Among metallic biomaterials, it is frequent to make comparisons between titanium alloys, cobalt-chromium alloys and stainless steels, and although stainless steels are generally superior in ductility and cyclic twist strength, they are weaker in biocompatibility and corrosion resistance comparing to titanium alloys, and weaker in wear resistance and stiffness comparing to cobalt-chromium alloys [51].

Furthermore, according to Holzapfel *et al.* [7], the much higher Young's modulus of 316L stainless steel compared with bone tissues can lead to stress shielding, and subsequent bone atrophy (Figure 6). The Young's modulus of bone can vary from 7 to 25

GPa, depending on the type of bone, location and age, whilst the 316L stainless steels modulus is, as stated, around 200 GPa [52].

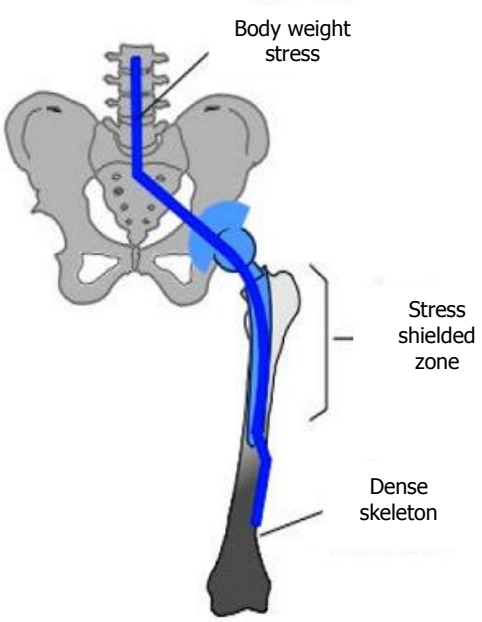

Figure 6 - Scheme of stress shielding after hip implant. After the implant insertion the body load is carried by both the bone and the implant, resulting in reduced stresses on the bone (represented in white), and consequent stress shielding. The dark area represents the overloading on the distal end of the femur. [49]

More importantly, there is always the risk of corrosion in the body environment, hence releasing compounds such as nickel, chromium or cobalt, and although these are not antigenic, they can stimulate hypersensitivity reactions through complex formation with proteins found in blood, and can even induce carcinogenesis [53]. In addition, as already referred, 316L stainless steel contains a considerable amount of nickel, which is widely recognized as a high risk element for incompatibility problems [54]. The presence of chromium, along with the traces of molybdenum and silicon, is also a downside as all of these elements tend to stabilize the ferritic phase, weaker than the desired austenitic phase.

1.2.2.3. Applications

Stainless steels were the first implant materials successfully employed in the surgical field, and today, along with titanium and its alloys, are widely encountered in dentistry, cardiology and orthopedics. Particularly, 316L stainless steel has been extensively used in biomedical applications such as bone plates, cranial plates, dental implants, spinal rods, joint replacement prostheses, cardiovascular stents and electric terminals, and as catheters [48, 51].

1.2.3. Adhesion

Under a chemical point of view, the notion of adhesion between materials derives from the establishment of interfacial bonds through forces at the interface of two surfaces, although it can also be employed when referring to the energy required to break the bond between both materials. High strength must be assured, thus it is required proper surface preparation, such as cleaned surface from contaminations, stable interface and suitable formation of chemical and physical bonds [55, 56]. Adhesive bonding technology has been developing along the last decades since it is crucial in areas such as aircraft and automobile industry [57].

1.2.3.1. Surface Treatments

When faced with two physically and chemically different materials, it is very challenging to join them together, hence the necessity to use surface treatments as a recourse to bonding strength. Substrate pretreatment is usually required in order to improve the adhesion between the surface and the coating. The substrate surface can be altered by removal of contaminants, by production of an oxide layer, by introduction of suitable chemical composition of the oxide, by introduction of chemical functions and by increase of surface roughness [57]. By roughness increasing, the contact area between both materials is increased, which in general improves the adhesion [58].

Chemical and mechanical treatments can improve the adhesion to metallic substrates including anodizing, surface grafting, flame treatment, microwave irradiation, sol-gel

coating, plasma treatments, grit-blasting and chromic-sulfuric acid treatment, depending on the application [56, 58].

Among these treatments there is silanization, one of the most commonly techniques used to bond different materials, and consists in the immobilization of organosilanes to surfaces. Silanes usually have the following structure:

$$X_3Si(CH_2)_n–Y \qquad \text{(eq. 1)}$$

where X is the hydrolysable group, Y is the functional group and n is typically 3. Because hydrolyzed molecules should not react with each other, silane solutions have very low concentrations (0.01–2%), avoiding the formation of oligomers. When the substrate comes in contact with the solution, silanol groups (SiOH) adsorb immediately to the substrate forming hydrogen bonds, followed by the drying and curing processes, where silanol groups react not only with metal hydroxyls forming a covalent bond, but also with each other, creating a siloxane network structure. This way, the silane treatment can be summarized in three steps: the silane hydrolysis, the silanization of the substrate (Figure 7) and the thermal curing of the silanized substrate [59]. The variables in this treatment must be controlled since they can affect the silane bonding to the surface. Solution concentration, solution pH and curing conditions are such examples. Thickness of the coupling agent layer is also an important factor to take into consideration since adhesion can suffer from too thin or thick layers, even though the optimum thickness varies according to the bonded material [59, 60]. Substrate surface roughness can also play its role, preventing the silane layer formation or breaking the ordered silane layers, meaning that smooth surfaces display beneficial properties [61].

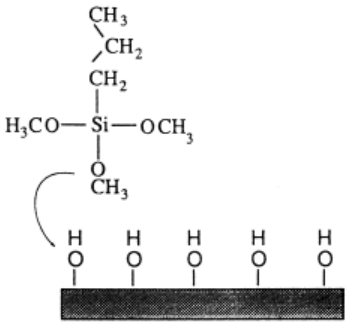

Figure 7 - The chemistry of a typical silane surface modification reaction. [6].

1.2.3.2. Adhesion measurement tests

Adhesion can be measured quantitatively and qualitatively and there are many mechanical and non-mechanical methods. Qualitative methods include x-ray diffraction, bend and scratch test, abrasion test, and tape test; and examples of quantitative methods are thermal method, nucleation test, capacitance test, scratch test, ultracentrifugal test, indentation test and direct pull-off method [62]. Pull-off adhesion test is widely used and attempts to evaluate the mechanical tensile strength of an adhesive [56]. Tests can also be divided into wear tests, related to the interfacial strength of coatings; thermal tests that influence adhesion strength during heating and cooling processes; shear tests that reflect the in-service conditions, and peel tests, in order to test the peel force. However, since there is still no ideal adhesion test that can satisfy all the requirements, the test should be chosen taking into account the materials and the applications.

1.2.4. Metal/Polymer interface

Coatings have demonstrated to give adequate protection to metals, and polymeric coatings have been largely used by the automotive industry, especially to prevent the formation of rust. This principle relies on the attack by the corrosive environment to the coating instead of the substrate, therefore reducing or delaying the substrate's corrosion rate [63, 64]. Accordingly, polymer/metal interfaces have been widely studied, and the main focuses in this field are generally the adhesion stability and the prevention of

degradation. This stability can be controlled by the amount of water present in the medium, as well as by the temperature, mechanical stress and the presence of defects [63]. Nazarov and Thierry [65] reported that the forces involved in the interaction of polymer and metal are van der Waals forces, ionic forces and donor/acceptor bonds. Although, when the sample is exposed to high humidity or immersed in an aqueous medium, water molecules replace polymer/metal bonds due to higher energy of interaction of the hydrogen bonds.

Some examples of polymeric coatings used onto 316L stainless steel are referred in Table 2. In fact, this steel is largely used in biomedical research for being one of the metallic materials most employed as an implant biomaterial. Moreover, it is also widely used in the industry field, although there is often the need of an application of a polymeric coating for corrosion protection. Conductive polymers such as polypyrrole, polyaniline and polythiophene, are defined as a promising method for this purpose [66].

Table 2 - Some examples of polymers coatings used onto 316L stainless steels and due purposes.

Polymer	***Purpose***	***Ref.***
polypyrrole	Corrosion prevention	[67, 68]
Parylene	Medical applications	[69]
allylamine	Cardiovascular stent coating	[70]
poly(5-nitroindole)	Corrosion prevention	[71]
chitosan and dextran	Biocompatibility enhancement	[72]
Chitosan	coating characterization	[73]
poly(ethylene glycol) (PEG)	Prevention of protein adsorption and bacterial adhesion	[74]

Despite the wide research on the interface between polymeric and metallic materials for corrosion prevention, this was not the motivation behind this work. Instead, PLLA films were chosen for the 316L stainless steel coating in order to promote bone regeneration, taking advantage of PLLA piezoelectric characteristic.

Chapter 2 - EXPERIMENTAL PROCEDURE

The experimental procedure of this work includes the following steps, briefly represented in the next flowchart (Figure 8):

1. characterization and polishing of 316L stainless steel substrates;
2. preparation and deposition of PLLA solution onto 316L stainless steel substrates by spin-coating: i) variation of the PLLA solution concentration and PLLA molecular weight to change the film thickness, ii) heat treatment of the PLLA films to change the polymer degree of crystallization;
3. immersion of PLLA films on phosphate buffered saline solution (PBS) for one week, one month and two months onto 316L stainless steel;
4. preliminary studies on substrate silanization using 3-(aminopropyl) triethoxysilane (APTES);
5. characterization of PLLA films onto 316L stainless steel substrates: microstructure, thickness and adhesion.

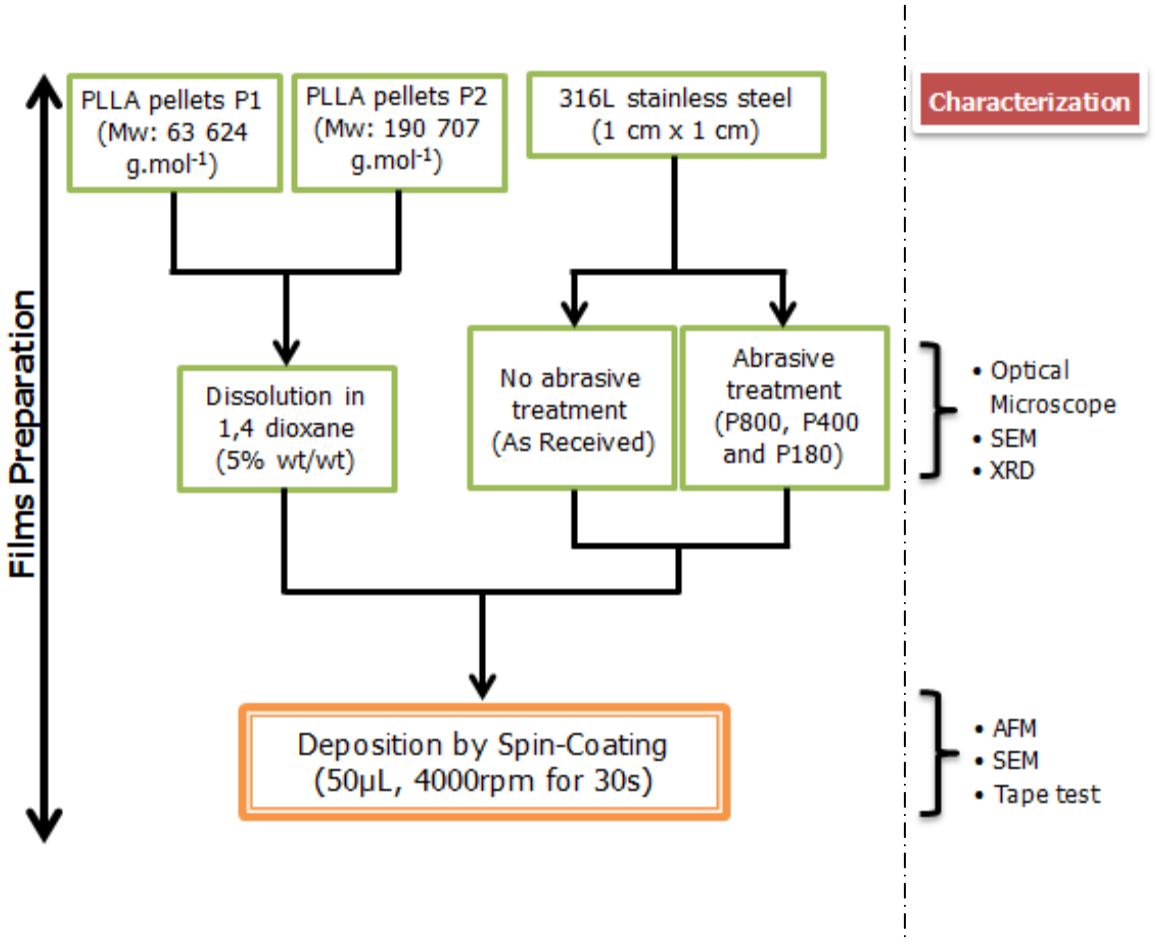

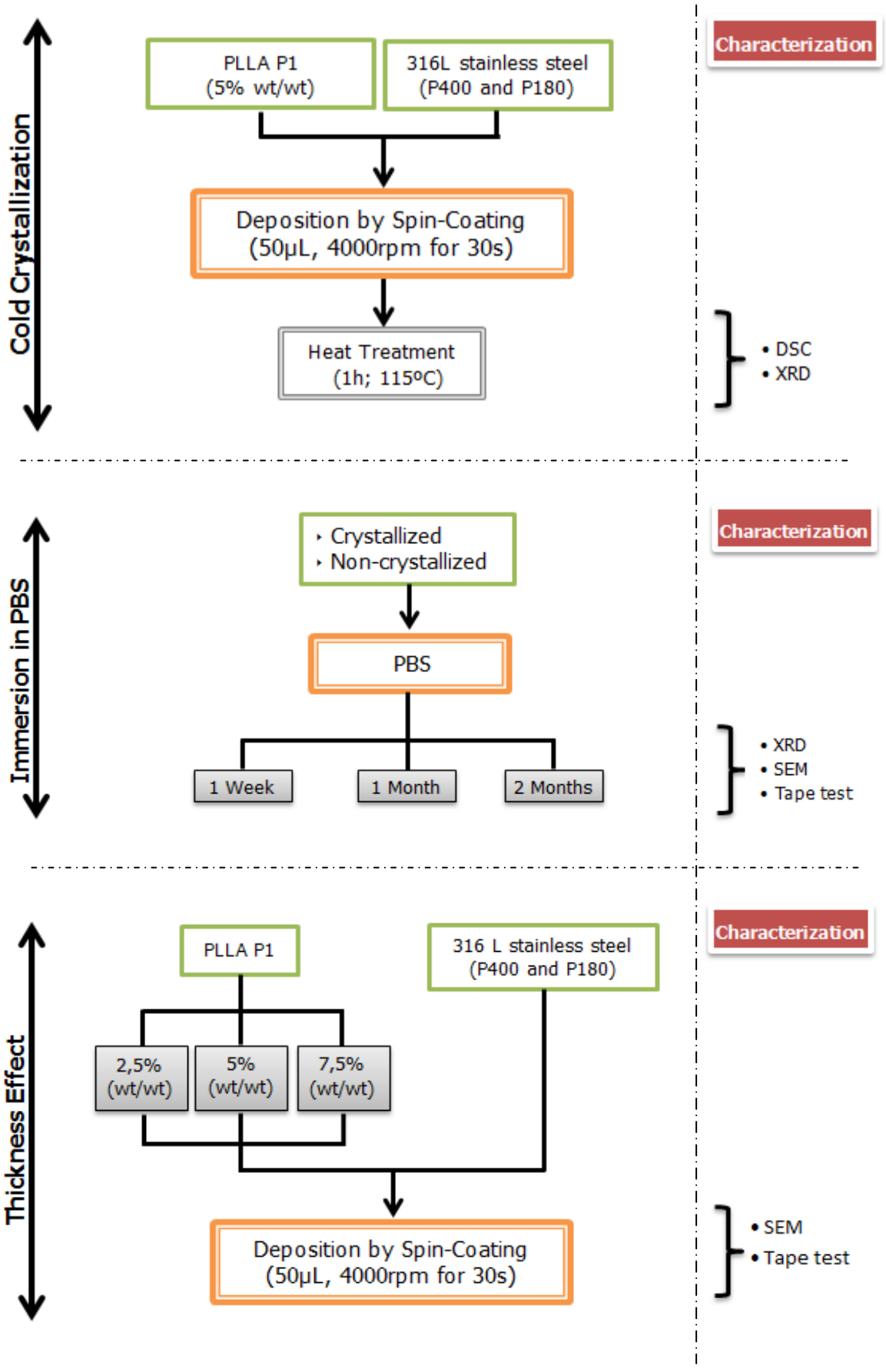
Cold Crystallization
PLLA P1
(5% wt/wt)
316L stainless steel
(P400 and P180)
Deposition by Spin-Coating
(50µL, 4000rpm for 30s)
Heat Treatment
(1h; 115ºC)
Characterization
• DSC
• XRD
Immersion in PBS
Crystallized
Non-crystallized
PBS
1 Week
1 Month
2 Months
Characterization
• XRD
• SEM
• Tape test
Thickness Effect
PLLA P1
316 L stainless steel
(P400 and P180)
2,5%
(wt/wt)
5%
(wt/wt)
7,5%
(wt/wt)
Deposition by Spin-Coating
(50µL, 4000rpm for 30s)
Characterization
• SEM
• Tape test

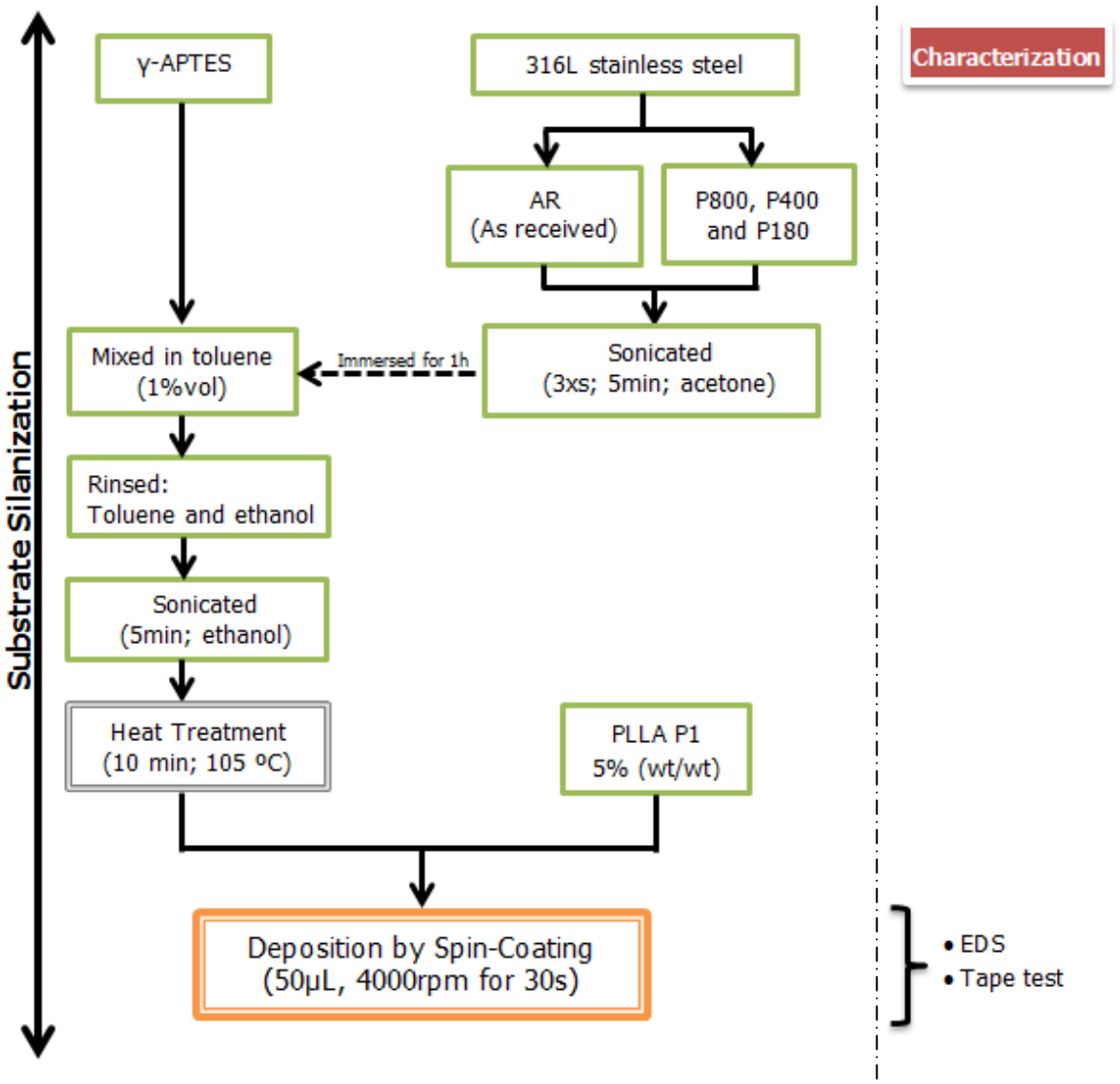

Figure 8 - Flowchart of the experimental procedure.

2.1. Materials

Starting materials were PLLA pellets (Purasorb® PL and Purasorb® PL38, both produced by Purac), which were dissolved in 1,4 dioxane (Panreac Quimica SA), and 316L stainless steel plates (AISI 316L from Goodfellow) that were cut into 1x1cm^2 samples. Waterproof abrasive disk paper with ISO grit designation P180 (coarser), P400 and P800 were used for the stainless steel abrasive treatment, and the reagents γ-APTES [(3-aminopropyl)triethoxysilane] and toluene (Panreac) were employed for the silanization treatment.

2.2. Preparation Techniques

2.2.1. Samples Preparation

PLLA pellets with two different molecular weights (63 624 g.mol^{-1} and 190 707 g.mol^{-1}) were dissolved with 5% (wt/wt) in 1,4 dioxane at 70ºC until completely dissolved (around 2h with magnetic stirring), 316L stainless steel plates were cut into 1x1cm^2 samples substrates. Some of these samples remained as received (AR) while some others were mechanically grinded with P180, P400 and P800 waterproof abrasive paper, using an automatic grinder/polisher (Struers RotoPol-11) (Figure 9). All of these treated samples suffered the same surface treatment for 15 minutes (8 minutes in one direction and 7 more minutes in another direction, represented in Figure 10, in order to produce increasing sample roughness) with applied force of 5N.

Figure 9 - Grinder/polisher used in this work.

Figure 10 - Simplified representation of the stainless steel sample aspect after the grinding treatment.

2.2.2. Film Deposition (spin-coating)

The PLLA films were deposited onto the stainless steel substrates by spin-coating (Chemat Technology spin-coater KW-4A) (Figure 11), under the following conditions: solution drop of approximately 50µL, spin velocity of 4000rpm and 30 seconds as spinning time.

Figure 11 - Outer side and inner side of the spin-coater used in this work.

The spin-coating technique is often used in thin polymeric films deposition and is an alternative to dip coating and spray coating since it can produce uniform coatings in a considerable large area [35, 75]. The typical process consists in the deposition of a drop of the polymer solution onto the substrate, followed by a high speed rotation of the substrate (Figure 12). Due to spinning, and therefore the centrifugal forces, the liquid flows radially covering the substrate, the solvent evaporates, and the excess is ejected off the edge [35, 76].

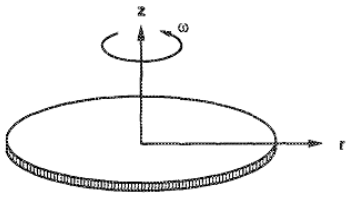

Figure 12 - Spin coating process model. [77]

2.2.3. In situ Crystallization

After the film deposition, the films were subjected to a cold-crystallization treatment, which was based and adjusted from some procedures in the literature [78] and expected to produce structural rearrangements as depicted in Figure 13. These samples were placed in the heater for 1h at 115 ºC, and afterwards left at room temperature in order to cool down at a non-controlled rate. Worth noting that, in this step, the samples were only grinded with P180 or P400 abrasive paper, and the chosen coating was the lower molecular weight PLLA solution (PLLA1).

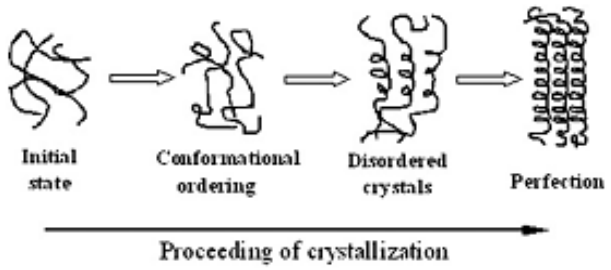

Figure 13 - Schematic diagram of sequential ordering at atomic scale during cold crystallization of PLLA. [79]

2.2.4. In-vitro degradation studies

Aiming to study the body environment degradation effect on the adhesion of PLLA films on stainless steel substrates crystallized and non-crystallized samples of PLLA1 deposited on the P400 and P180 grinded stainless steel substrates were immersed in 10 mL of PBS solution (P3813, Sigma) and kept at 37,4 ºC for one week, one month or two months.

2.2.5. Thickness Effect

The film thickness was expected to vary between PLLA solutions with different molecular weights and concentrations. Two different molecular weight PLLA pellets have

been used: PLLA1 with a molecular weight of 63 624 $g.mol^{-1}$ and PLLA2 with a molecular weight of 190 707 $g.mol^{-1}$. The thickness effect was also studied varying the solution concentration of the polymer PLLA1. PLLA1 solutions with 2,5% (wt/wt) and 7,5% (wt/wt), besides the 5% (wt/wt), were prepared and deposited by spin-coating on P180 or P400 surface treated stainless steel substrates.

2.2.6. Silanization

Notwithstanding the physical surface treatment, a chemical one was performed, namely silanization. As previously described, this is a methodology that aims at the adsorption of the silanol groups to the stainless steel substrates, expected to improve the adhesion of the coatings to the substrate. Therefore, both the non-grinded samples and the samples grinded with P800, P400 and P180 abrasive paper, were sonicated three times in acetone for 5 minutes each, before being soaked in a solution of 1 vol% APTES in toluene. After 1h, the samples were rinsed in toluene and ethanol, and then sonicated in ethanol for 5 minutes. Finally, the samples were dried in air and kept at around 100-105 ºC for 10 minutes in the stove. This procedure was adapted from the one described in Yoshioka *et al.* [80], although the heating step was skipped since the attempts showed a burning effect on the stainless steel substrates.

2.3. Characterization Technique

2.3.1. DSC

The differential scanning calorimetry (DSC) is a technique used for the determination of the thermal events (exo and endothermic), such as phase transformations, glass transitions, crystallizations or melting, that occur on materials when heated or cooled. The method is based on the comparison of the material behavior with another material not subjected to changes at those temperatures. Therefore, in a typical polymer DSC curve it is possible to observe the exothermic reactions (crystallization and oxidation) and the endothermic changes (glass transition, melt and degradation) [81].

In order to address the crystallization behavior a DSC assay was underwent by Tecoflex SG80A in the temperature range of 20 ºC to 200 ºC, with a heating rate of 10 ºC/min.

2.3.2. AFM

The atomic force microscopy (AFM) allows to generate surface topographic maps, permitting the detection of changes after surface treatment, being also able to measure surface roughness [82], contributing in this way with valuable information to adhesion strength. In the scope of this work, this technique was used to monitor the morphology of differently treated stainless steel substrates and films, and to measure their roughness, owing to the fact that the rugosimeter proved to be unfeasable. AFM was equally to assess the crystallization state of some samples.

2.3.3. SEM

The scanning electron microscopy (SEM) is one of the most used surface analysis techniques, and its principle is based on the intensity detection of the secondary electrons and X-rays emitted after the sample is bombarded with electrons, consequently generating a three dimensional surface image [83]. In doing so, this approach was widely used in this research, usually with an accelerating voltage of 25 kV, especially to survey morphology modifications after the samples were immersed in PBS. In addition, for the purpose of thickness measurement, cross-sections of the samples were visualized. Figure 14 shows the samples prepared for SEM visualization.

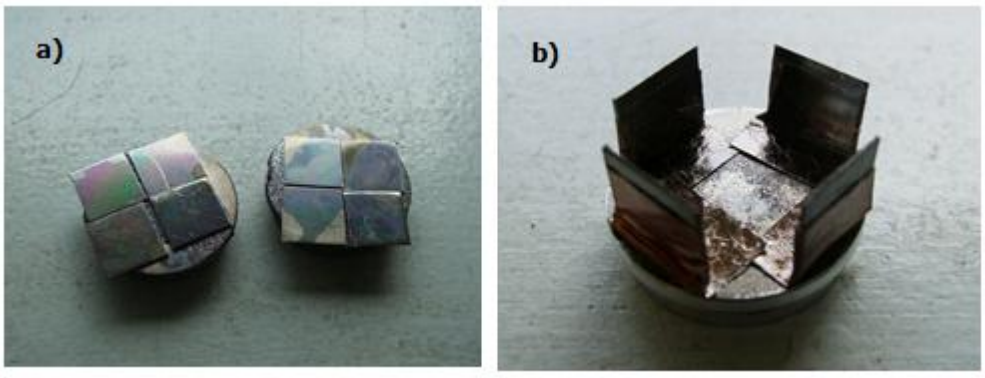

Figure 14 - SEM samples preparation for **a)** surface visualization and **b)** cross-section visualization.

2.3.4. XRD

X-ray diffraction (XRD) method is a commonly used technique to analyze structural features of materials, such as crystallographic systems, crystallite size, crystallographic orientations, information of phase compositions, among others [84]. In this work, XRD analysis (with Rigaku Geigerflex Dmax-C apparatus) was conducted to assess the crystallinity of stainless steel and PLLA films in general, and in particular, crystallized and non-crystallized films after PBS immersion.

2.3.5. Tape Test

There are many qualitative and quantitative tests available for adhesion measurements. Among all, the chosen test for the scope of this work was the tape test, following the standard test method for measuring adhesion, ASTM D3359. This test method was developed to measure the adhesion of coating films to metallic substrates, through the application of a pressure-sensitive tape. Accordingly, a crosshatch pattern was performed with a diamond cutter tool on the polymeric film (Figure 15a), and the pressure-sensitive tape was applied covering the entire sample surface. The tape was then removed quickly by pulling it off with an angle of 180º (Figure 15b) and the adhesion was assessed using a scale from 0 to 5, where 5 represents the highest level of adhesion whilst 0 represents the lowest (Figure 16).

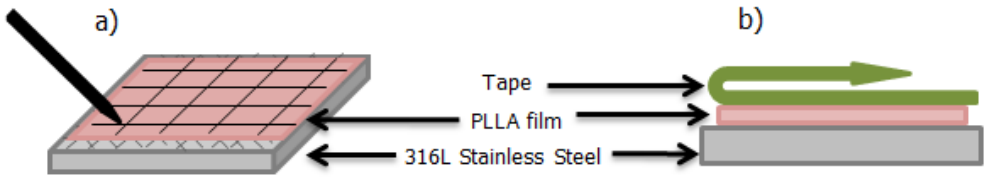

Figure 15 - Schematic representation of the tape test: **a)** performing a crosshatch pattern, followed by **b)** the application and removal of the tape with an angle of 180º.

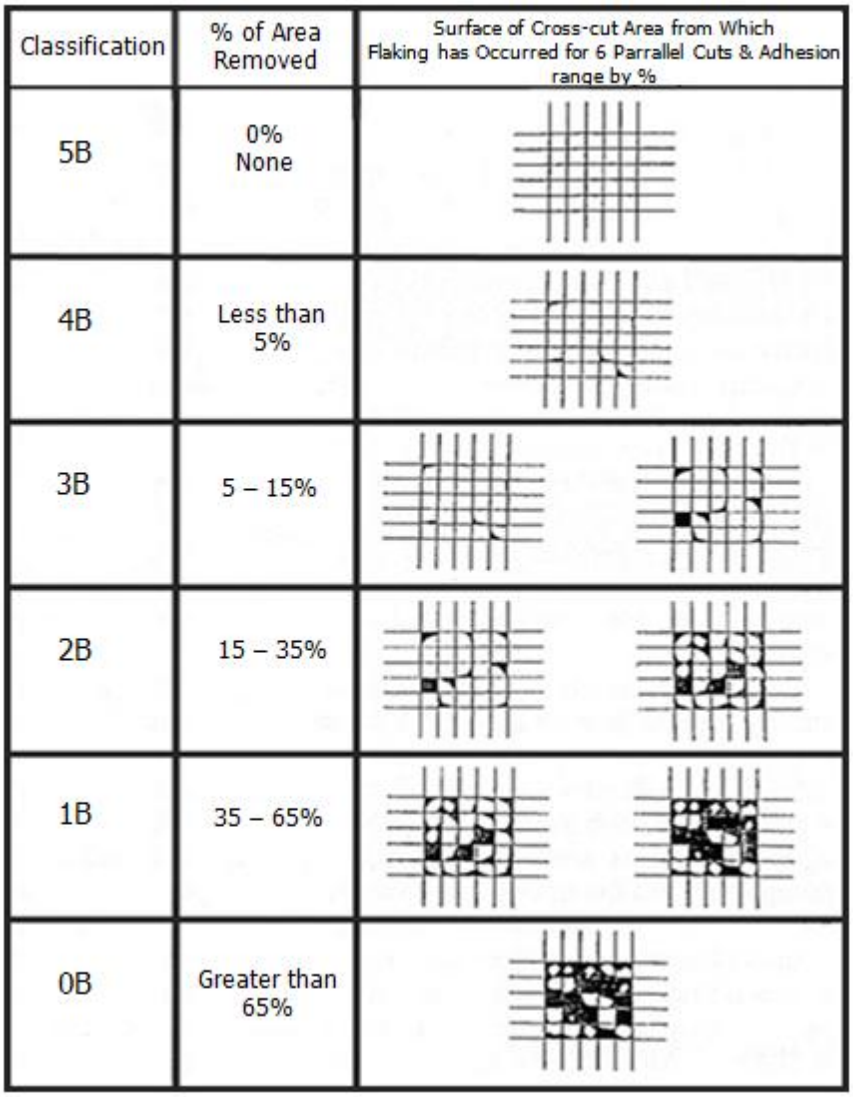

Figure 16 - Classification of the removed area (represented in black) according to the ASTM D3359.

Chapter 3 - RESULTS AND DISCUSSION

3.1. Substrate characterization

The 316L stainless steel substrates were grinded with P800, P400 and P180 abrasive papers in order to increase substrate roughness and to study its effect on PLLA film adhesion. As seen in the optical micrographs (Figure 17), the stainless steel sample without abrasive treatment presents a uniform smooth surface as opposed to the other samples, which were submitted to physical treatment and as a consequence reveal obvious scratched surfaces. It is also noticeable that the scratches density increases with the increase of the average particle diameter of the abrasive papers (P800 > P400 > P180), with obvious increasing when comparing surfaces grinded with P800 and P400 (samples 2 and 3, respectively). In accordance, the scratches density is highest in the surface grinded with P180 paper (sample 4) comparing to sample 3.

This effect is corroborated by the SEM analysis (Figure 18), where the first sample's surface (1) is obviously different comparing to the other three samples, since there was no physical treatment. The SEM micrograph displays the characteristic grained surface of steels in which some grain and grain boundaries can be observed and no scratches are noted. The grinded samples exhibit clear scratches, being the scratch density increased for the samples grinded with P400 and P180 abrasive papers (3 and 4, respectively) as expected. As the density of scratches increases the grained microstructure becomes more difficult to be observed.

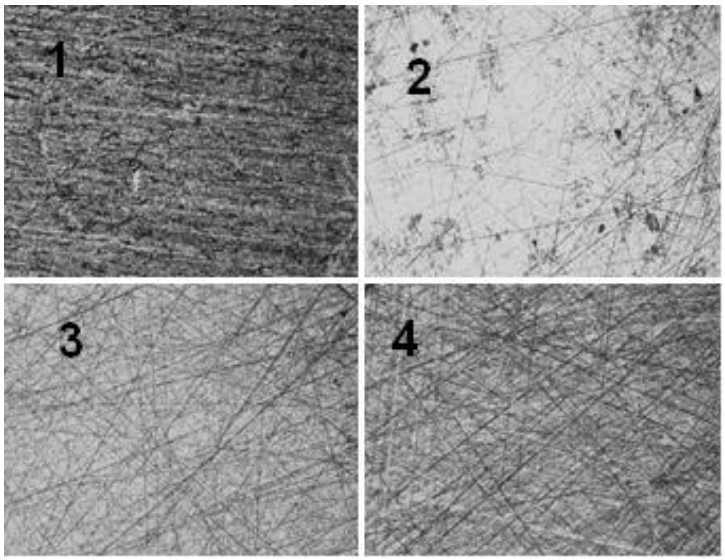

Figure 17 - Optical micrographs of 316L stainless steel samples: **(1)** as-received; and grinded with **(2)** P800; **(3)** P400 and **(4)** P180 abrasive papers.

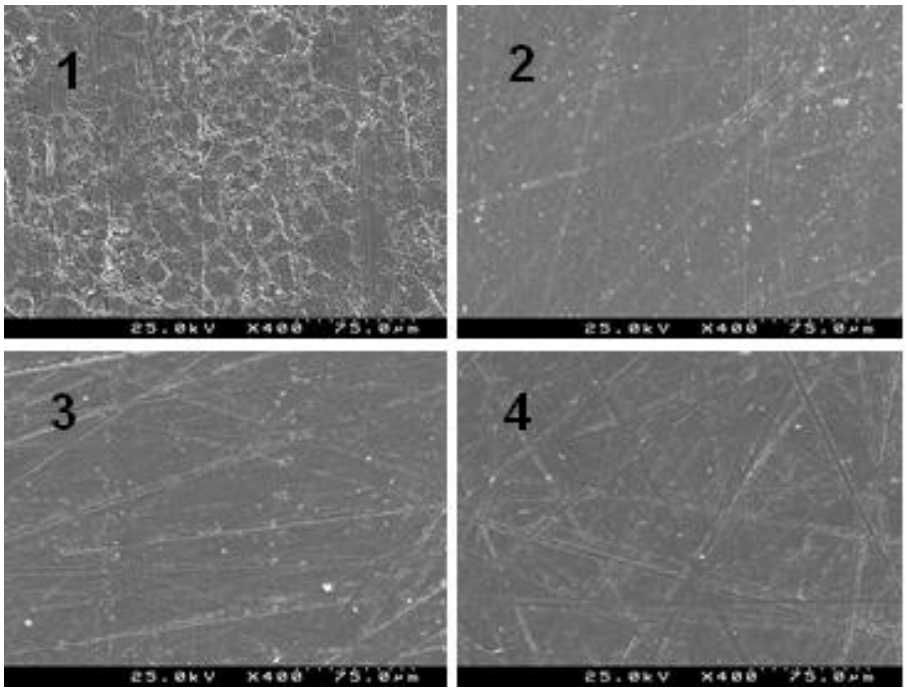

Figure 18 - SEM pictures of 316L stainless steel samples: **(1)** as-received; and grinded with **(2)** P800; **(3)** P400 and **(4)** P180 abrasive papers.

As a complementary characterization technique, the x-ray diffraction analysis of the stainless steel substrates to assess the phase composition was conducted. Figure 19 shows the XRD patterns of the stainless steel used in this work. As expected, peaks correspondent to the austenitic and ferritic phases are present. Austenitic phase peaks occur at approximately 2θ = 43º, 2θ = 51º and 2θ = 75º, associated to the diffraction plans (111), (200) and (220), respectively. Ferritic phase peaks were detected around 2θ = 45º and 2θ = 65º, associated to the diffraction plans (110) and (200), respectively. No other phases were detected. Figure 20 shows the XRD of the 316L stainless steel found in the literature [85] that exhibits a very similar XRD pattern to the one under study in this work.

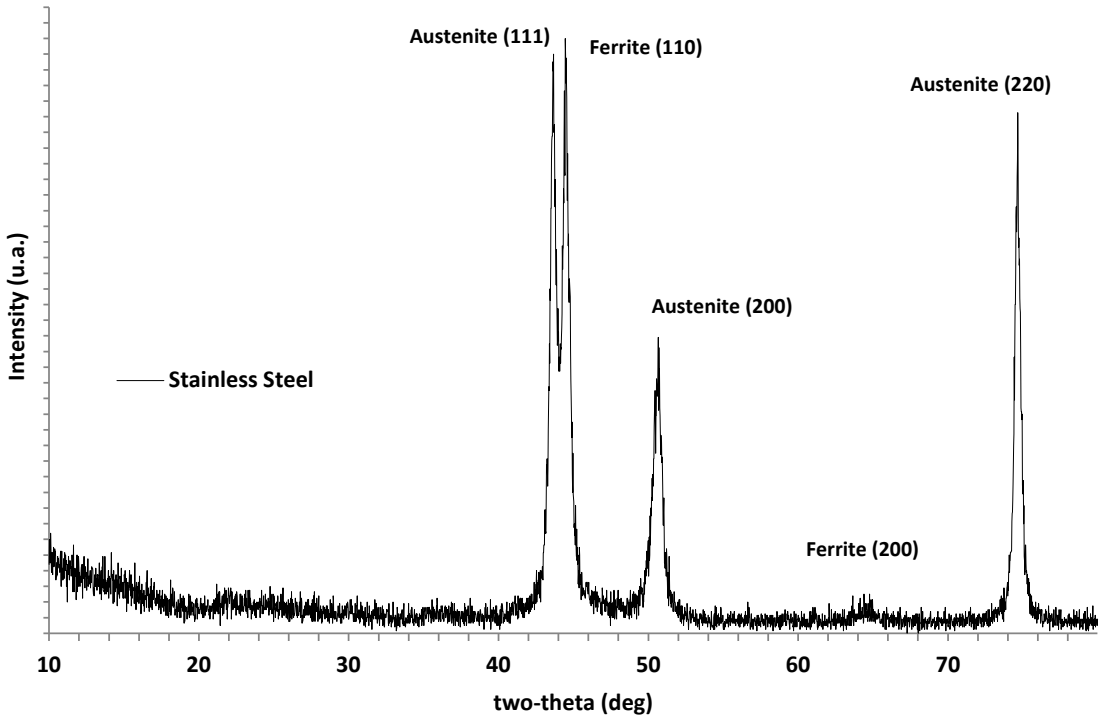

Figure 19 - X-ray diffraction of the 316L stainless steel used in this work.

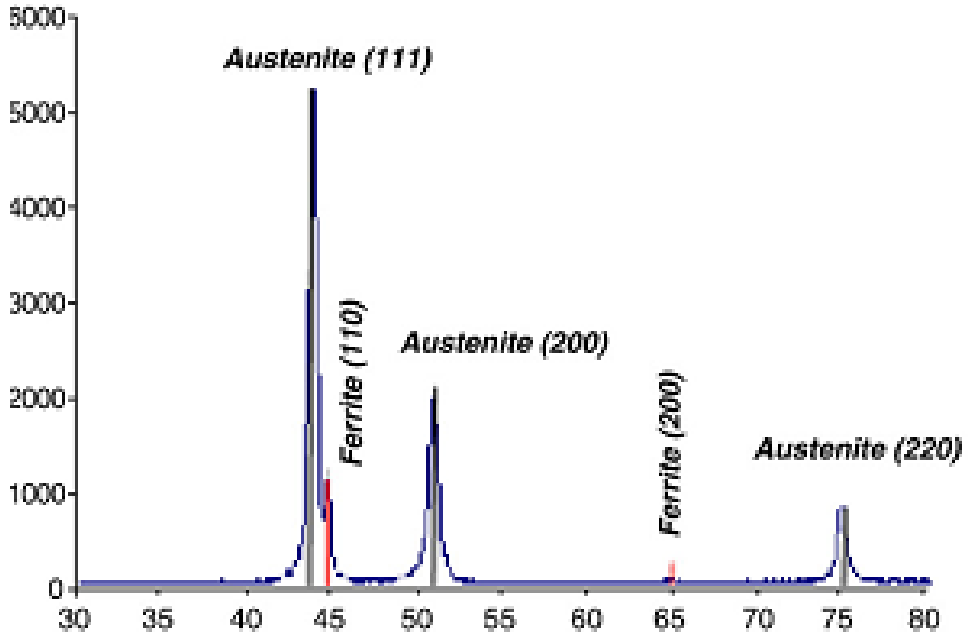

Figure 20 - X-ray diffraction of the 316L stainless steel reported in the literature. [85]

Atomic Force Microscopy (AFM) was used as an additional tool for surface imaging and roughness quantification. The results here presented correspond to just some samples. Unfortunately, due to an apparatus malfunction not all the samples were analyzed. Consequently, for substrate characterization only samples grinded with P180 and P400 abrasive paper have been analyzed. The topography images are presented in Figure 21 along with their roughness measurements and the mean roughness of three different areas. The AFM roughness measurements confirm that the higher the abrasive paper particle diameter, the rougher is the substrate surface; surfaces grinded with P180 abrasive paper have a mean roughness of 131±15 nm, while the substrates grinded with P400 abrasive paper have 116±15 nm, being possible to make such affirmation.

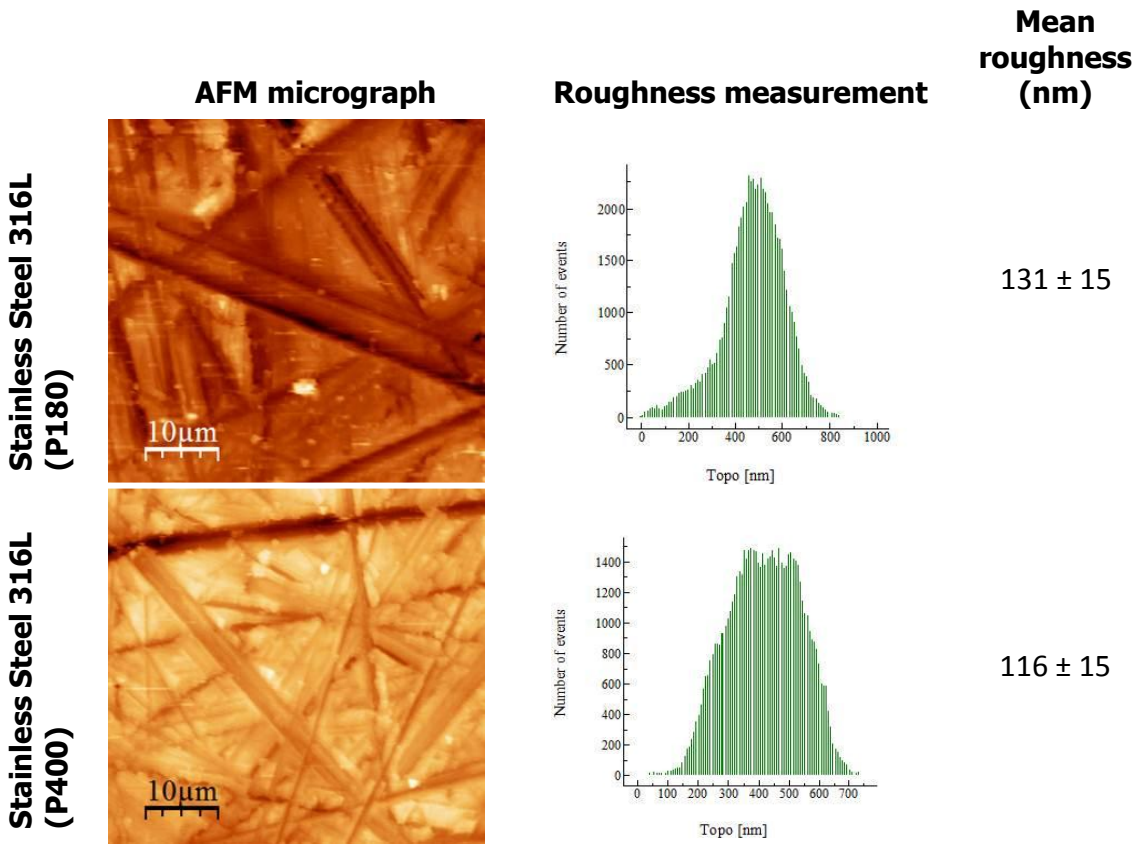

Figure 21 - AFM topography images, roughness measurements and mean roughness values of stainless steel samples grinded with P180 and P400 abrasive papers.

A well-known alternative surface treatment for steels is silanization, via which the surface of the steel substrate is functionalized with Si terminations to improve, by chemical reaction, the adhesion of the coating to the substrate. Preliminary studies were attempted in this work and after the silanization treatment SEM-EDS analysis was performed with SEM apparatus. Figure 22 represents EDS spectra of the substrate without any treatment whilst Figure 23 represents the substrate after this treatment. In both figures, peaks of stainless steel main constituents (iron, chromium and nickel) were detected. Nevertheless, in Figure 23 another peak is visible, and corresponds to the silicon element, which clearly suggests the presence of silicon on the treated substrate.

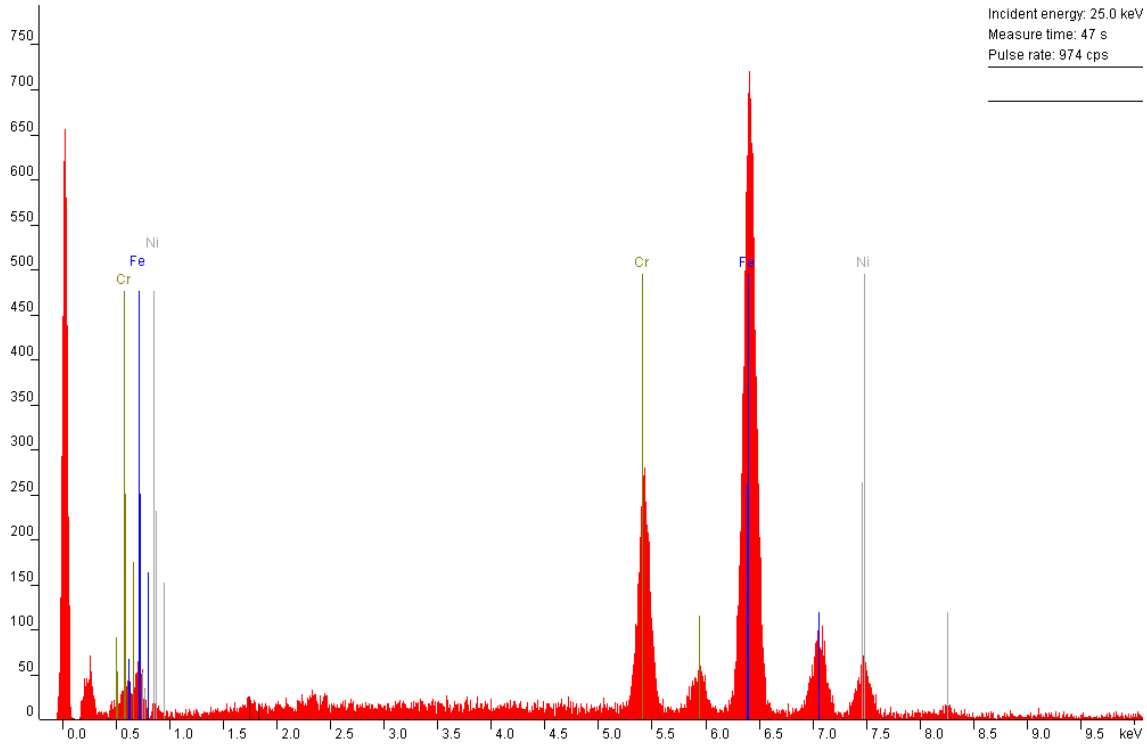

Figure 22 - EDS spectra of a non-silanized stainless steel substrate.

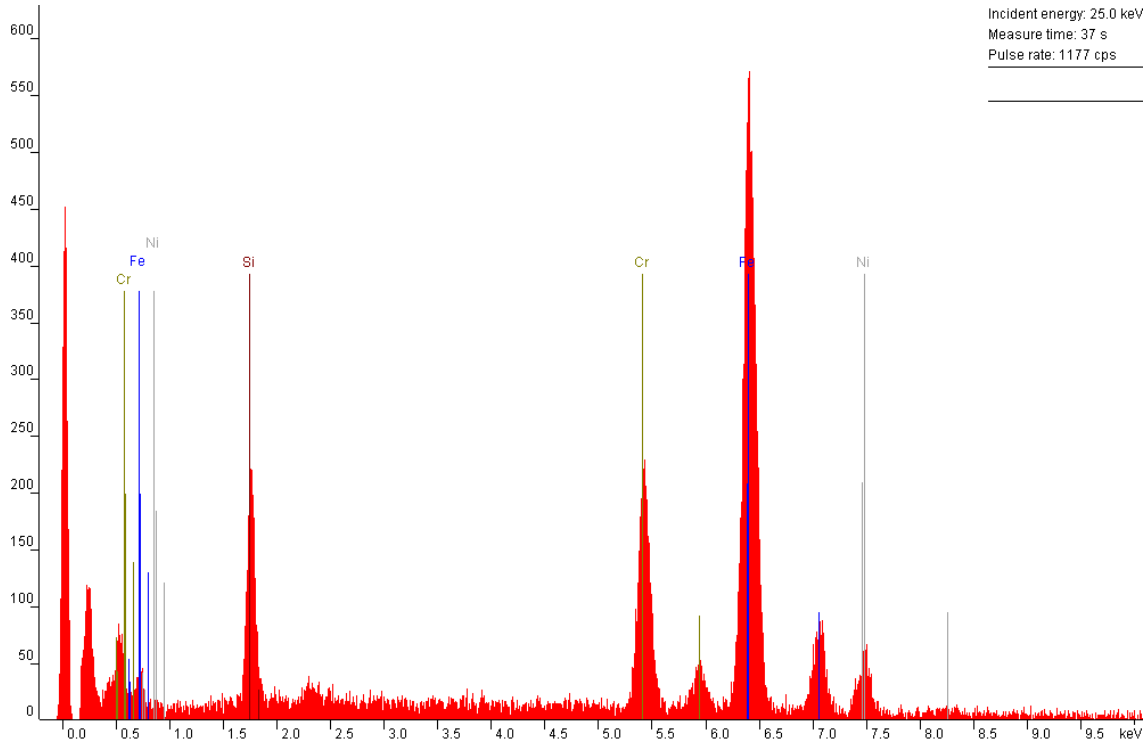

Figure 23 - EDS spectra of a stainless steel substrate after silanization treatment, demonstrating a clear silicon peak.

3.2. Film characterization

Figure 24 shows the SEM micrographs of the differently treated stainless steel substrates (both as received and grinded with the abrasive papers) coated with PLLA films. The film is clearly transparent since the scratches from the samples' surfaces are still visible, although not that perceptible as seen in Figure 18, due to the film covering.

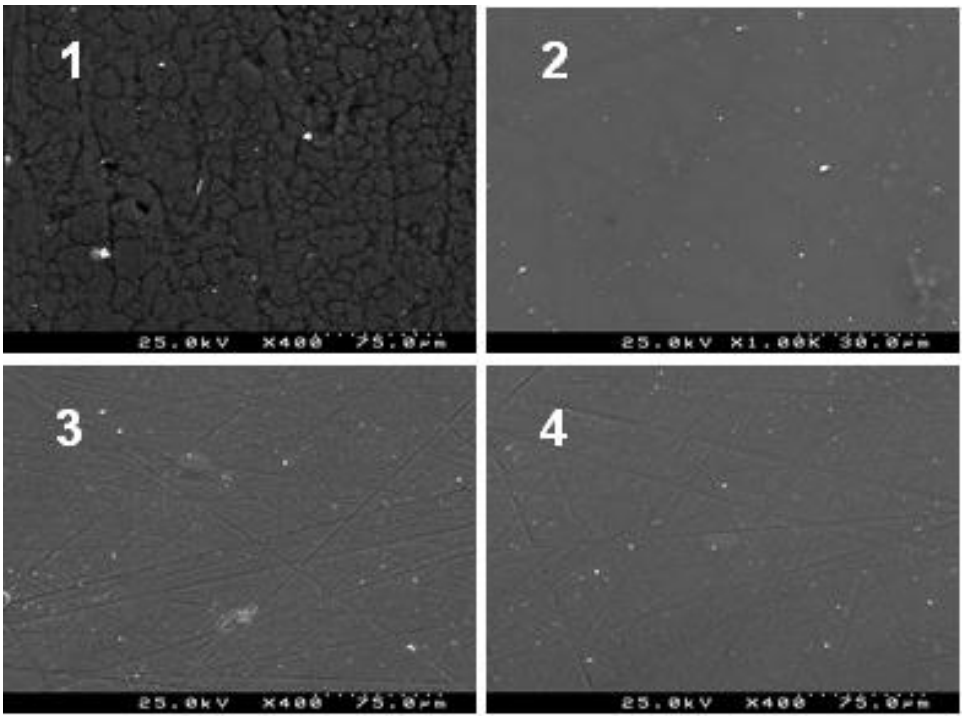

Figure 24 - SEM micrographs of PLLA1 coated stainless steel samples: **(1)** as-received; and grinded with **(2)** P800; **(3)** P400 and **(4)** P180 abrasive papers.

The film thickness was measured for the two PLLA films used in this work by SEM.

Figure 25 illustrates the cross-section views of the studied samples. For a better visualization a cut in the middle of every sample was made and the thickness measured.

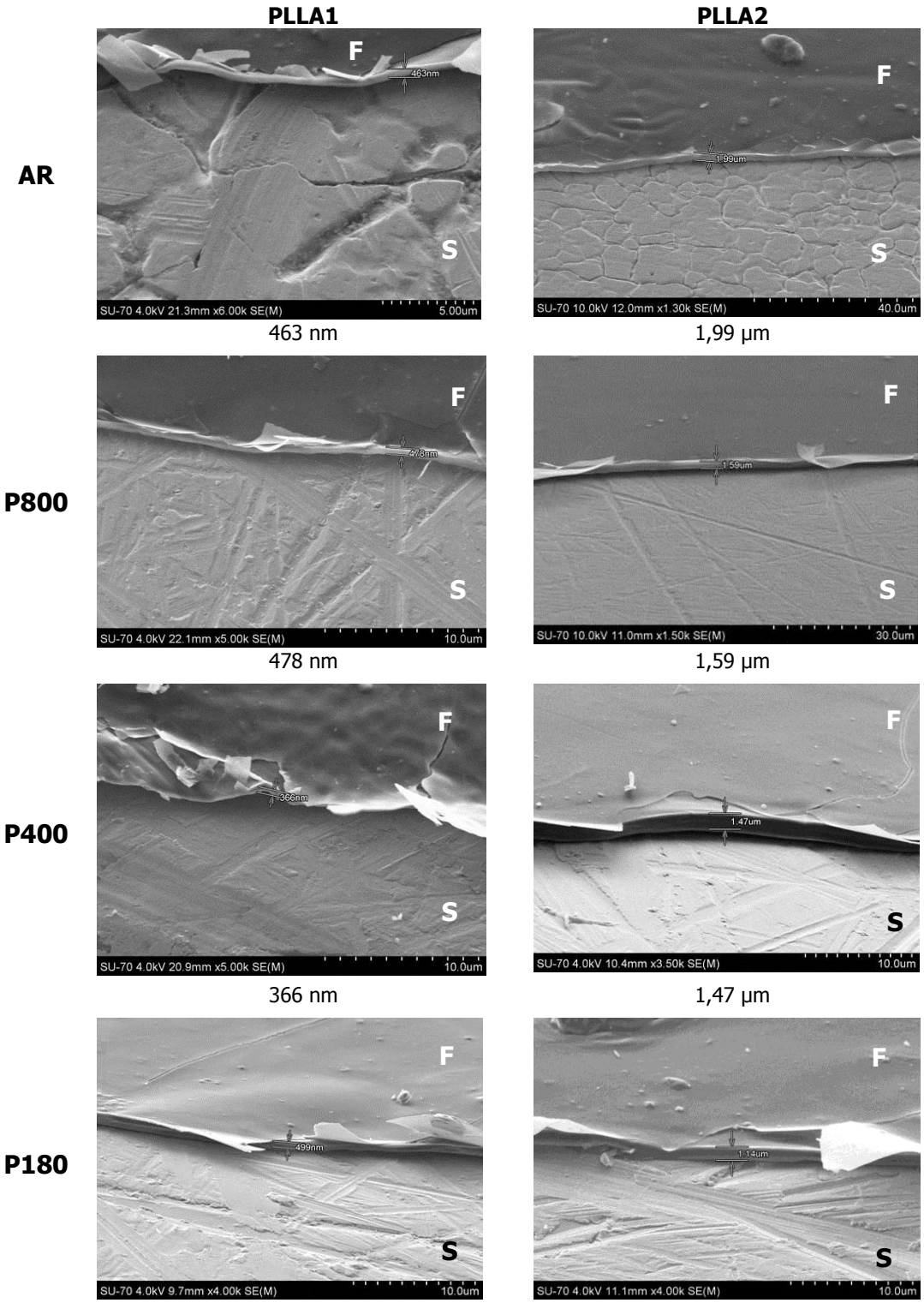

463 nm | 1,99 µm

478 nm | 1,59 µm

366 nm | 1,47 µm

499 nm | 1,14 µm

Figure 25 - SEM cross-section micrographs of the as-received (AR) and grinded with the P800, P400 and P180 abrasive papers stainless steel samples, coated with PLLA with two different molecular weights: PLLA1 with the lowest molecular weight, and PLLA2 with the highest molecular weight. Thickness values were measured with the SEM software, and are indicated below the correspondent sample. "F" indicates the film, and "S" indicates the stainless steel substrate.

There is an obvious difference between PLLA films derived from different polymer molecular weights. As expected, PLLA films prepared from the higher molecular weight (PLLA2) are thicker when compared to the PLLA films prepared from the lower molecular weight (PLLA1). PLLA1 films have thickness in the range of around 400 nm, while the PLLA2 ones have thickness between 1 and 2 μm. In terms of film thicknesses there is no obvious difference between the films deposited on treated and non-treated substrates. If there are differences, they are relatively small and a more accurate process should be used. For some samples it was possible to visualize an additional layer on the top of the PLLA film, possibly due to several carbon depositions.

The effect of the film thickness on the film adhesion to the substrate was also studied by changing the polymer concentration, besides the molecular weight of the polymers. Accordingly solutions of different concentrations of the same PLLA (PLLA1) were prepared, namely solutions of 2,5% (wt/wt), 5% (wt/wt) and 7,5% (wt/wt) were synthesized and deposited by spin coating on the 316L substrates grinded with P400 and P180 abrasive paper. SEM micrographs of these films are shown in Figure 26. The measured film thickness for the 2,5% (wt/wt) solution is in the range of 200 nm, around 400 nm for the films of the 5% (wt/wt) solution and approximately 1μm for the films derived from 7,5% (wt/wt) solution. Comparing these results, there is a confirmation that the higher the solution concentration, the thicker is the film.

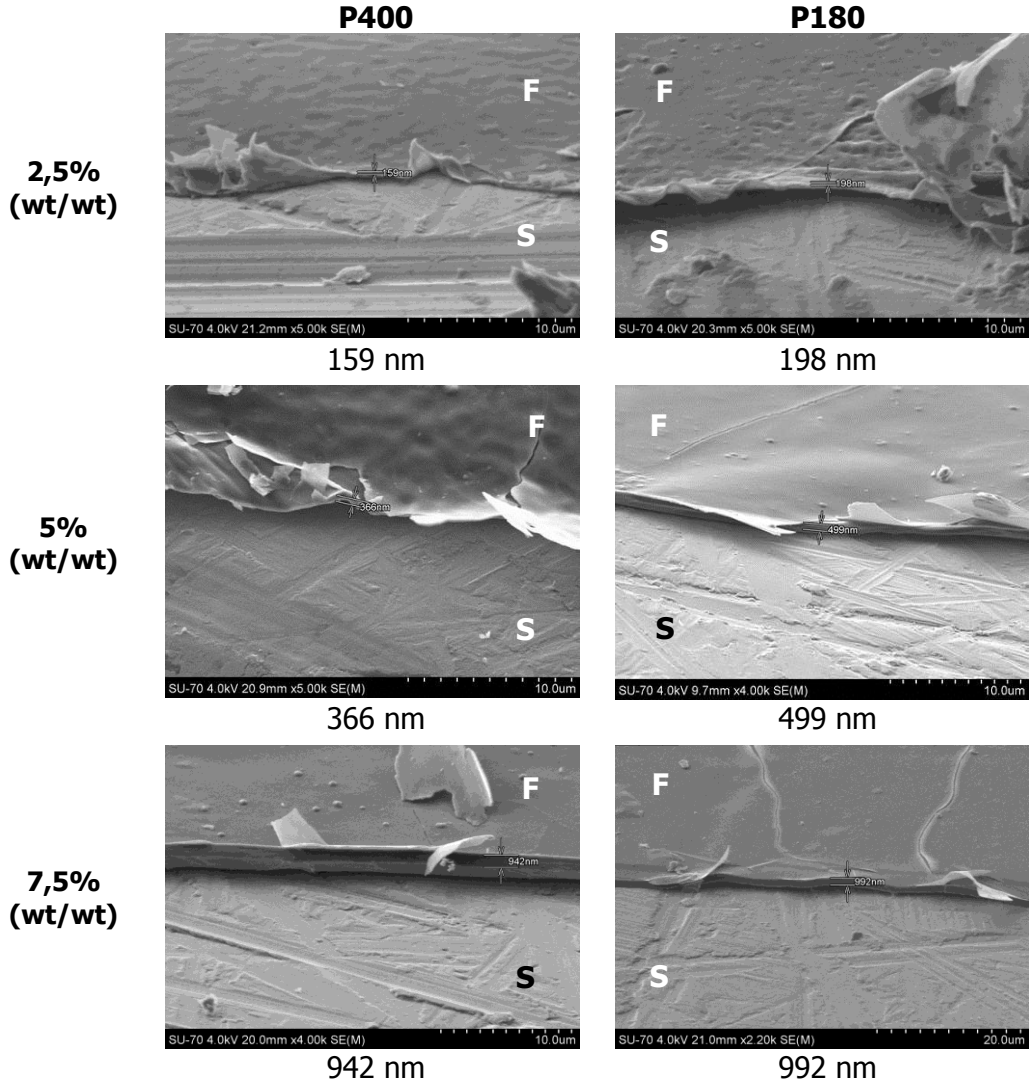

Figure 26 - SEM cross-section micrographs of stainless steel samples grinded with P180 and P400, and coated with different solution concentrations of the same PLLA: 2,5% (wt/wt), 5% (wt/wt) and 7,5% (wt/wt). Thickness values were measure with the SEM software, and are indicated below the correspondent sample. "F" indicates the film and "S" indicates the stainless steel substrate.

As already mentioned, AFM was a helpful tool to survey film surface imaging and to quantify the film surface roughness. Figure 27 presents the topography images along with their roughness measurements and the mean roughness for some of these films (PLLA1 films stainless steel samples grinded with P180 and P400); the film thickness is in the range of 400 nm. As the roughness of the substrate increases the roughness of the surface of the film increases as well, from 61 to 90 nm. Within this film thickness the film

roughness mimics the substrate surface roughness. When comparing these results with those represented in Figure 21 it is clear that the non-coated substrates have more visible scratches than the samples coated with the films, in which the scratches seem to be more blurred, hence corroborating the results from SEM previously presented (Figure 18 and Figure 24). Indeed substrates coated with the PLLA films present lower mean roughness than the non-coated stainless steel substrates: for the P180 grinded sample, the coated samples analyzed present a mean roughness of 90±9 nm while the substrates have 131±15 nm, and for the P400 grinded sample, the coated samples present a mean roughness of 61±3 nm against 116±15nm of the non-coated grinded substrates.

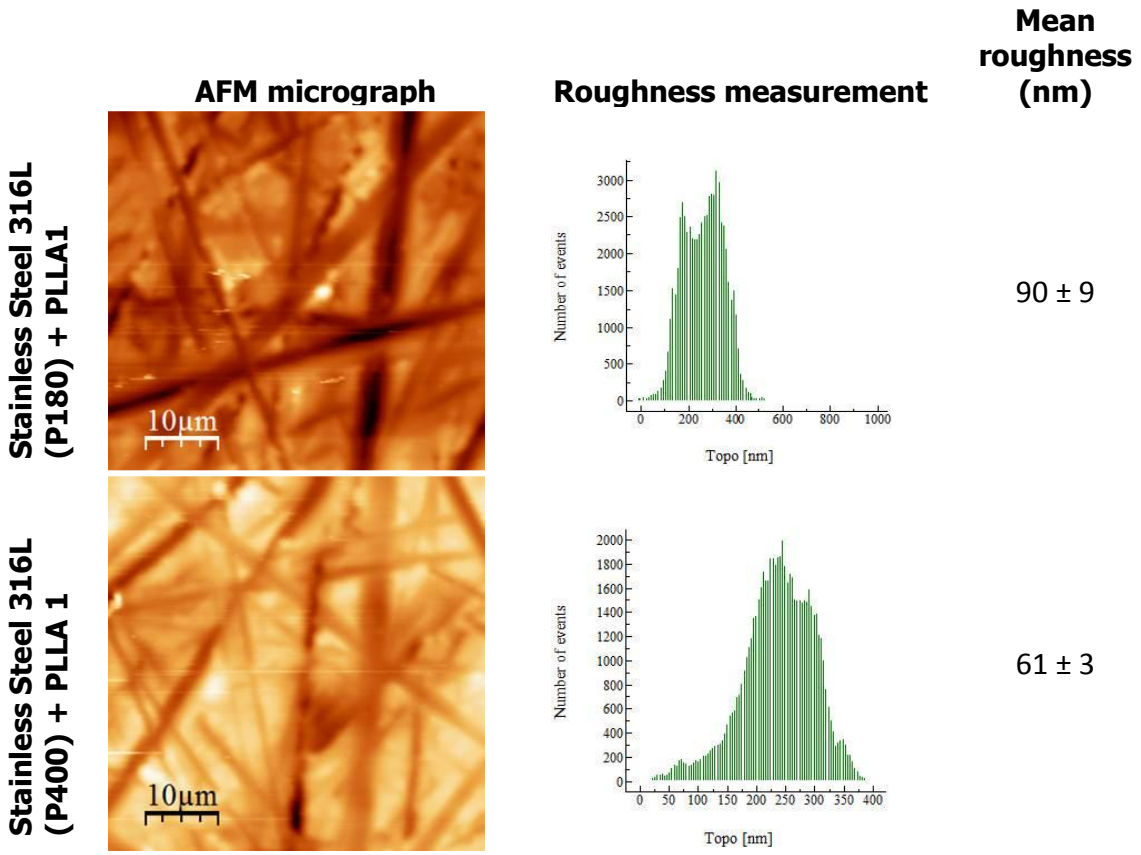

Figure 27 - AFM topography images and roughness measurements of stainless steel substrates grinded with P180 and P400 coated with the lower molecular weight PLLA (PLLA1).

In order to assess the effect of the crystallization on the adhesion of the PLLA films to the stainless steel substrates differential scanning calorimetry was performed to study the thermal behavior of PLLA1 films. Owing to the fact that manual detachment of PLLA films from stainless steel substrates is very difficult, films for the calorimetric studies were deposited and crystallized onto Pyrex glass substrates.

The DSC measurements were made at the heating rate of 10 ºC/min, in the temperature range of 25 ºC < T < 200 ºC, described in Figure 28. It was observed that melting temperature (Tm) for the non-crystallized film was 176 ºC while for the crystallized ones was 178 ºC.

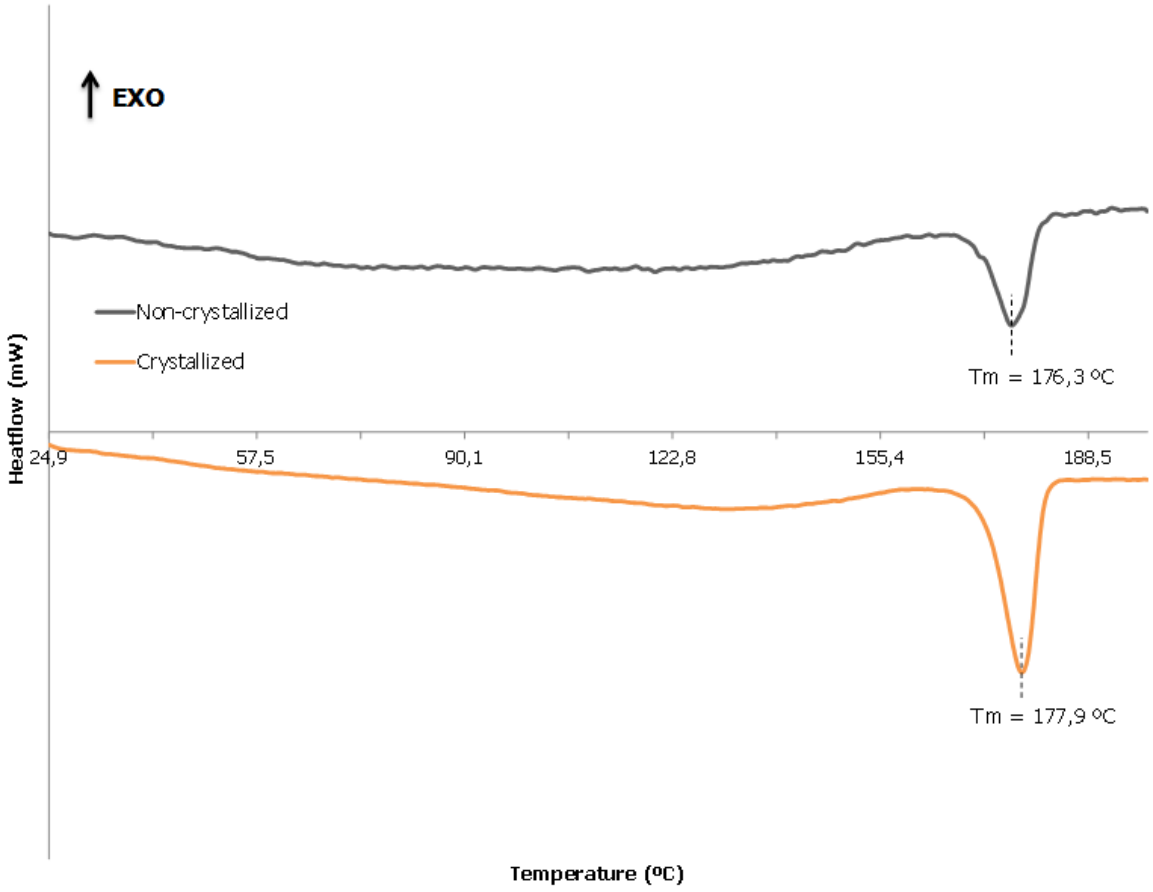

Figure 28 - DSC curves of crystallized and non-crystallized PLLA1 films on glass substrates. Melting temperatures were measured, being 176 ºC for the non-crystallized film and 178 ºC for the crystallized one.

Although the distinction between the areas of both peaks is evident, the crystallinity degree (X_c) was calculated for each sample, using the following equation:

$$X_c = \frac{\Delta H_f}{\Delta H_f^0} \times 100$$

where ΔH_f represents the measured enthalpy of fusion and ΔH_f^0 is the calculated enthalpy of fusion of a wholly crystalline material (93 J/g for PLLA) [86]. Therefore, the calculated crystallinity degree of the non-crystallized sample is around 20% whilst the crystallinity degree of the crystallized sample is 36%.

Figure 29 shows the XRD patterns of crystallized and non-crystallized PLLA films prepared under the current work. Both spectra are characterized between 10 and 80º 2θ and both exhibit the correspondent peaks of the stainless steels substrates. However for films crystallized at 115 ºC the XRD spectrum presents a new diffraction peak at around 17º, characteristic of PLLA. Similar peaks at 17º (2θ) have been reported in the literature [87, 88]. Likewise, Cao *et al* [88] observed the increasing of the intensity of this peak with the increasing temperature of the heat treatment.

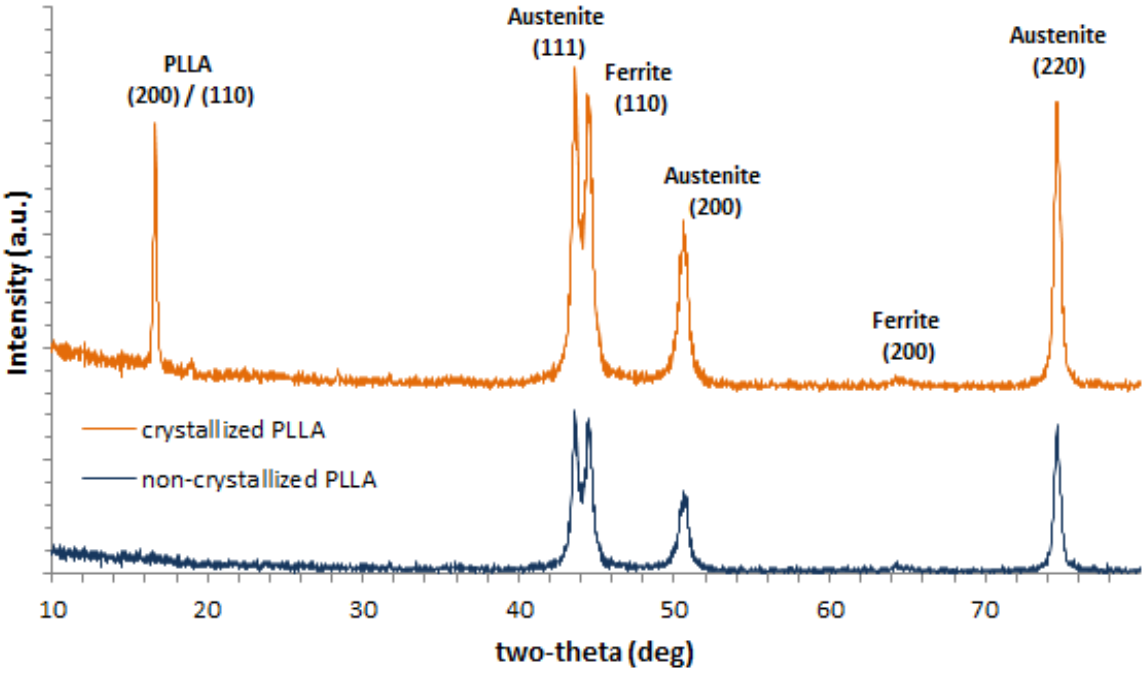

Figure 29 - XRD patterns of crystallized and non-crystallized PLLA films deposited on stainless steel substrates.

Figure 30 shows the SEM micrographs of the samples immersed in PBS and in almost all the samples a surface crystallization process was detected. It is possible that upon an uncontrolled drying the NaCl present in the PBS solution or any other residue induced a surface crystallization on the PLLA films.

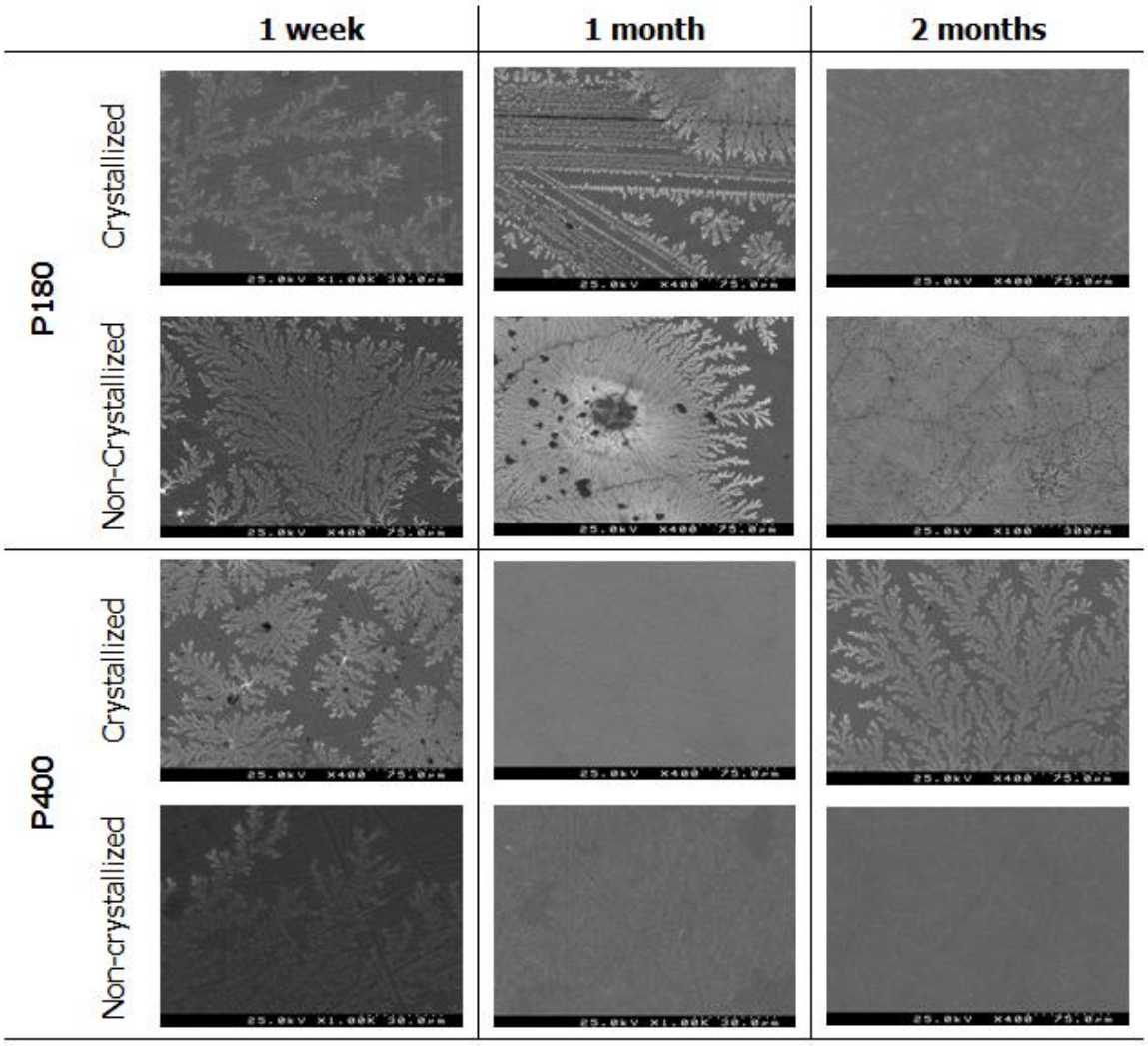

Figure 30 - SEM micrographs of crystallized and non-crystallized PLLA1 on 316L stainless steel substrates grinded with P180 or P400 abrasive papers that were immersed in PBS for one week, one month and two months.

3.3. Adhesion Measurements

Tape test based on the ASTM D3359 norm was performed in the as-received and the surface treated stainless steel samples coated with PLLA films. The effect of substrate surface roughness, film thickness, polymer molecular weight, and polymer degree of crystallization was assessed and the results presented and discussed in the next section.

Table 3 exhibits the main results related with the effect of the substrate roughness and polymer molecular weight, i.e. film thickness.

PLLA1 films (with molecular weight 63 624 $gmol^{-1}$) deposited on the stainless steel substrate without physical treatment, i.e. as received (AR) show a very poor adhesion, since the polymer coating was completely removed during the tape test. In opposition, films on the top of the scratched substrate surfaces (P180 and P400) present a better adhesion performance in terms of the tape test. The films on substrates grinded with the P800 abrasive paper, that showed the lowest scratch density, present the worst results of adhesion between the treated substrates. From these results the abrasive treatment proved to be beneficial in terms of film adhesion.

Concerning the polymer molecular weight, i.e. film thickness, the adhesion is improved when comparing non scratched with scratched substrates. However for PLLA2 films (with molecular weight 190 707 $gmol^{-1}$), for which the thickness is higher, the best adhesion is observed for the substrates treated with P800 and decreases for the substrates treated with P400 and P180. These results clearly indicate that the film thickness plays a crucial role and that the effect of the substrate roughness on the adhesion of the PLLA films depends on the film thickness. The results also indicate that there is a thickness limit or an ideal thickness that should be determined for each polymer and substrate roughness.

Overall, the PLLA1 (with the lowest molecular weight) provided the best performance when comparing to PLLA2. For this molecular weight polymer (PLLA1), the optimized adhesion performance was obtained, as expected, for the highest scratch concentration, i.e., samples grinded with the P180 abrasive paper, followed by the samples grinded with P400 abrasive paper coated with the same film solution.

Table 3 - Tape test results of PLLA films with two different molecular weights (PLLA1 and PLLA2), on 316L stainless steel substrates, as received (AR) and after grinded (P800, P400 and P180), according to the ASTM D3359. Percentage of area removed indicated between brackets. The film thickness is around 400 nm for PLLA1 and 1-2 μm for PLLA2.

		AR	P800	P400	P180
PLLA1	S1	0B (>65%)	4B (<5%)	4B (<5%)	5B (0%)
	S2	0B (>65%)	3B (5-15%)	3B (5-15%)	5B (0%)
	S3	0B (>65%)	3B (5-15%)	3B (5-15%)	5B (0%)
	S4	0B (>65%)	3B (5-15%)	4B (<5%)	
PLLA2	S1	0B (>65%)	4B (<5%)	3B (5-15%)	2B (15-35%)
	S2	0B (>65%)	4B (<5%)	2B (15-35%)	1B (35-65%)
	S3	0B (>65%)	4B (<5%)	3B (5-15%)	1B (35-65%)
	S4				2B (15-35%)

The effect of the film thickness on the adhesion performance to the stainless steel substrates was further assessed for PLLA1 films prepared with different solution concentration and the results are summarized on

Table 4. Films processed from the 2,5% (wt/wt) solution, with average thickness of 200 nm do not present any pealing for both grinded substrates surfaces, providing the best results in terms of adhesion performance.

Concerning 5% (wt/wt) solution, films with an average thickness of 400 nm films show a similar behavior as the previous ones for the substrates grinded with P180, since PLLA films was not detached from the substrate. However, in the case of the substrates grinded with P400 these PLLA films peeled off.

For the case of the thicker films, derived from the 7,5% (wt/wt) solution, independent on the polishing treatment of the substrate PLLA films were detached from the substrate during the tape test. The obtained results are a clear evidence of the role of the film thickness; as the film thickness increases, the ability to be detached from the substrate increases, i.e., film adhesion decreases. As the previous results (Table 2) there is a thickness limit, above which the adhesion of the films decreases, independently of the roughness of the substrate.

Table 4 - Tape test results of two different PLLA1 solutions [7,5% and 2,5% (wt/wt)] deposited onto stainless steel samples grinded with P400 and P180 abrasive paper. Percentage of area removed indicated between brackets.

		P180	***P400***
2,5% (wt/wt)	S1	5B (0%)	5B (0%)
	S2	5B (0%)	5B (0%)
	S3	5B (0%)	5B (0%)
5% (wt/wt)	S1	5B (0%)	4B (<5%)
	S2	5B (0%)	3B (5-15%)
	S3	5B (0%)	3B (5-15%)
7,5% (wt/wt)	S1	2B (15-35%)	4B (<5%)
	S2	2B (15-35%)	3B (5-15%)
	S3	1B (35-65%)	3B (5-15%)

Based on these previous results and because not all the samples showed proper adhesion the film to the substrate, some films were selected to proceed with further characterizations, namely the crystallization and PBS degradation effect. Therefore, PLLA1 films on stainless steel substrates grinded with P400 and P180 abrasive paper were crystallized under the conditions previously described. These samples, along with non-crystallized samples, were then submitted to degradation in PBS for one week, one month and two months. The tape test was assessed after these times, and the results are shown in Table 5.

Table 5 - Tape test results of three crystallized (C) and non-crystallized (NC) PLLA1 on stainless steel substrates, grinded with P400 and P180 abrasive paper, that were immersed in PBS for 1 week, 1 month and 2 months. Percentage of area removed indicated between brackets.

		P400		P180	
		Crystallized	Non-crystallized	Crystallized	Non-Crystallized
1 week	S1	3B (5-15%)	2B (15-35%)	2B (15-35%)	3B (5-15%)
	S2	2B (15-35%)	2B (15-35%)	2B (15-35%)	3B (5-15%)
	S3	2B (15-35%)	1B (35-65%)	2B (15-35%)	2B (15-35%)
1 month	S1	2B (15-35%)	2B (15-35%)	2B (15-35%)	2B (15-35%)
	S2	1B (35-65%)	2B (15-35%)	1B (35-65%)	1B (35-65%)
	S3	1B (35-65%)	1B (35-65%)	1B (35-65%)	0B (>65%)
2 months	S1	0B (>65%)	0B (>65%)	0B (>65%)	0B (>65%)
	S2	0B (>65%)	0B (>65%)	0B (>65%)	0B (>65%)
	S3	0B (>65%)	0B (>65%)	0B (>65%)	0B (>65%)

According to these results, there were no significance differences between the crystallized and non-crystallized samples. However, there is a visible loss of adhesion with the immersion time. After the first week in PBS the film adhesion was noticeably weaker, tending to aggravate with the increasing of immersion time. After two months in PBS, all the films were completely detachment from the substrates, independently on the substrate roughness.

The film was probably detached from the substrate due to water penetration under the coating, which can induce changes in the chemical composition and microstructure [89].

As an attempt to clarify the adhesion outcome after the insertion of silicon onto the substrate, the tape test was carried out on the silanized samples. The preliminary results are presented in Table 6.

Table 6 - Tape test results of the silanized substrates, both as received (AR) and after grinded (P800, P400 and P180), coated with PLLA1. Percentage of film area removed indicated between brackets.

	AR	***P800***	***P400***	***P180***
S1	0B (>65%)	0B (>65%)	2B (15-35%)	4B (<5%)
S2	0B (>65%)	0B (>65%)	2B (15-35%)	4B (<5%)
S3	0B (>65%)	0B (>65%)	1B (35-65%)	3B (5-15%)

For the silanized substrates not only the samples with the smoothest surface (AR) but also the samples grinded with the P800 abrasive paper scored poorly on this test, since there was a total delamination of the film. In contrast, the samples grinded with the P400 and P180 abrasive papers presented better results. Indeed, the film of the P180 samples showed almost optimal results, with a small percentage of detached polymeric film. However, it is self-evident that these findings on the whole are by no means as good as the samples without the presence of silicon (Table 3). Although preliminary, these results raise the question whether the silanization of 316L stainless steel substrates would in fact improve the adhesion between the PLLA and the substrate. This requires more systematic studies and a clear identification of the silanization of the substrate surface.

Chapter 4 - CONCLUSIONS

In this work, biocompatible stainless steel 316L substrates were successfully coated with biocompatible, biodegradable and piezoelectric PLLA films, after the modification of the steel surface, in order to improve film adhesion. The adhesion of the polymeric films to the substrate was assessed by a qualitative test, the so called tape test, following the ASTM D3359 standard.

Stainless steel 316L substrates were polished with different abrasive papers (P800, P400 and P180) to increase the substrate's roughness. A first set of preliminary tests on the silanization of the steel substrates was conducted aiming at the functionalization of the substrates and their effect on the adhesion of PLLA films.

In addition, two PLLA solutions with different molecular weights (PLLA1 and PLLA2) were used and PLLA films deposited onto the stainless steel substrates by spin-coating. The thickness of the films prepared under the same conditions increased with the increasing polymer molecular weight. The degree of crystallinity of the films was changed by changing the heat treatment.

It was observed that the adhesion of PLLA films on stainless steel 316L substrates:

1. is improved with the increasing of the substrate roughness;
2. depends on the film's thickness; although in this work a critical thickness has not been identified, it is shown that the adhesion decreases for thick films (> 1 micron);
3. doesn't depend on the degree of crystallinity of the PLLA films;
4. decreases with immersion in PBS and with the immersion time.

Overall, the combination of the PLLA films and 316L stainless steel substrates appears to be suitable for potential biomedical applications.

Future Work

Despite the fact that this work presented successful outcomes, there were some limitations. Therefore the following ideas are suggested:

- to explore the possibility of other adhesion measurement tests, preferentially quantitatively; and
- to proceed to functionalization of the substrate surface.

REFERENCES

1. Abe, A., K. Dušek, and S. Kobayashi, *Biopolymers - Lignin, Proteins, Bioactive Nanocomposites*. Advances in Polymer Science. Vol. 232. 2010: Springer.

2. Geetha, M., et al., *Ti based biomaterials, the ultimate choice for orthopaedic implants – A review.* Progress in Materials Science, 2009. **54**(3): p. 397-425.

3. Igwe, J., et al., *Nanostructured Scaffolds for Bone Tissue Engineering*. Active Implants and Scaffolds for Tissue Regeneration. Vol. 8. 2011, Israel. 169–192.

4. Zhang, Q., et al., *Fluorescent PLLA-nanodiamond composites for bone tissue engineering.* Biomaterials, 2011. **32**(1): p. 87-94.

5. Lendlein, A. and A. Sisson, *Handbook of Biodegradable Polymers*2011, Germany: Wiley-VCH. 426.

6. Ratner, B.D., *Biomaterials Science - An Introduction to Materials in Medicine* 2nd ed2004, London: Elsevier Academic Press.

7. Holzapfel, B.M., et al., *How smart do biomaterials need to be? A translational science and clinical point of view.* Advanced Drug Delivery Reviews, 2012.

8. Verma, D. and N.D.S. University, *Design of Polymer-biopolymer-hydroxyapatite Biomaterials for Bone Tissue Engineering: Through Molecular Control of Interfaces*2008: North Dakota State University.

9. Mano, J.F., et al., *Bioinert, biodegradable and injectable polymeric matrix composites for hard tissue replacement: state of the art and recent developments.* Composites Science and Technology, 2004. **64**(6): p. 789-817.

10. Kuhn, L.T., *6 - BIOMATERIALS*, in *Introduction to Biomedical Engineering (Second Edition)*2005, Academic Press: Boston. p. 255-312.

11. Wuisman, P.I. and T.H. Smit, *Bioresorbable polymers: heading for a new generation of spinal cages.* European Spine Journal, 2006. **15**(2): p. 133-48.

12. Rasal, R.M., A.V. Janorkar, and D.E. Hirt, *Poly(lactic acid) modifications.* Progress in Polymer Science, 2010. **35**(3): p. 338-356.

13. Sodergard, A. and M. Stolt, *Properties of lactic acid based polymers and their correlation with composition.* Progress in Polymer Science, 2002. **27**: p. 1123-1163.

14. Yotoriyama, T., et al., *Surface characterization of thin film induced by He ion-beam irradiation into PLLA.* Surface and Coatings Technology, 2005. **196**(1-3): p. 383-388.

15. Turner, J.F., et al., *Characterization of drawn and undrawn poly-L-lactide films by differential scanning calorimetry.* Journal of Thermal Analysis and Calorimetry, 2004. **75**: p. 257–268.

16. O'Connor, A., A. Riga, and J.F. Turner, *Determination of crystalline content gradients in cold-drawn poly-L-lactic acid films by DSC.* Journal of Thermal Analysis and Calorimetry, 2004. **76**: p. 455–470.

17. Chen, J.P. and C.H. Su, *Surface modification of electrospun PLLA nanofibers by plasma treatment and cationized gelatin immobilization for cartilage tissue engineering.* Acta Biomaterialia, 2011. **7**(1): p. 234-43.

18. Xu, L., et al., *Surface modification of poly-L-lactic acid films by electrostatic self-assembly to promote vascular smooth muscle cells growth.* Frontiers of Materials Science in China, 2007. **1**(4): p. 388-394.

19. Wang, Y. and J. Cai, *Enhanced cell affinity of poly(l-lactic acid) modified by base hydrolysis: Wettability and surface roughness at nanometer scale.* Current Applied Physics, 2007. **7**: p. e108-e111.

20. Cui, Y.L., et al., *Biomimetic surface modification of poly(l-lactic acid) with chitosan and its effects on articular chondrocytes in vitro.* Biomaterials, 2003. **24**(21): p. 3859-3868.

21. Nair, L.S. and C.T. Laurencin, *Biodegradable polymers as biomaterials.* Progress in Polymer Science, 2007. **32**(8-9): p. 762-798.

22. Yanagida, H., et al., *Cell adhesion and tissue response to hydroxyapatite nanocrystal-coated poly(L-lactic acid) fabric.* Journal of Bioscience and Bioengineering, 2009. **108**(3): p. 235-43.

23. Kakalis, A. and C. Panayiotou, *Characterization of interfaces formed between thin, poly(l-lactic acid) polymer films and quartz crystal microbalance, sensor substrates with high frequency impedance analysis.* Sensors and Actuators A: Physical, 2011. **169**(1): p. 59-65.

24. Luckachan, G.E. and C.K.S. Pillai, *Biodegradable Polymers- A Review on Recent Trends and Emerging Perspectives.* Journal of Polymers and the Environment, 2011. **19**(3): p. 637-676.

25. Deplaine, H., J.L.G. Ribelles, and G.G. Ferrer, *Effect of the content of hydroxyapatite nanoparticles on the properties and bioactivity of poly(l-lactide) – Hybrid membranes.* Composites Science and Technology, 2010. **70**(13): p. 1805-1812.

26. Kanemura, C., S. Nakashima, and A. Hotta, *Mechanical properties and chemical structures of biodegradable poly(butylene-succinate) for material reprocessing.* Polymer Degradation and Stability, 2012. **97**(6): p. 972-980.

27. Nampoothiri, K.M., N.R. Nair, and R.P. John, *An overview of the recent developments in polylactide (PLA) research.* Bioresource Technology, 2010. **101**(22): p. 8493-501.

28. Luca Fambri, C.M., Kemal Kesenci, and Erhan Piskin, *Biodegradable Polymers.* Integrated Biomaterials Science,, 2002: p. 119-187.

29. Lam, K.H., et al., *Biodegradation of porous versus non-porous poly(L-lactic acid) films.* Journal of Materials Science: Materials in Medicine, 1994. **5**: p. 181-189.

30. Handolin, L., et al., *The effect of low-intensity pulsed ultrasound on bone healing in SR-PLLA rod fixed experimental distal femur osteotomy in rat.* Journal of Materials Science: Materials in Medicine, 2007. **18**(6): p. 1239-45.

31. Pistner, H., et al., *Poly(l-lactide): a long-term degradation study in vivo: Part II: physico-mechanical behaviour of implants.* Biomaterials, 1994. **15**(6): p. 439-450.

32. Ma, Z., et al., *Cartilage tissue engineering PLLA scaffold with surface immobilized collagen and basic fibroblast growth factor.* Biomaterials, 2005. **26**(11): p. 1253-1259.

33. Middleton, J.C. and A.J. Tipton, *Synthetic biodegradable polymers as orthopedic devices.* Biomaterials, 2000. **21**: p. 2335-2346.

34. Fu, J., et al., *Early Stage Interplay of Microphase Separation and Crystallization in Crystalline-Coil Poly(L-lactic acid)-block-polystyrene Thin Films.* Macromolecules, 2005. **38**: p. 5118-5127.

35. Xu, L. and A. Yamamoto, *Characteristics and cytocompatibility of biodegradable polymer film on magnesium by spin coating.* Colloids and Surfaces B: Biointerfaces, 2012. **93**: p. 67-74.

36. Chen, Y., et al., *In vitro behavior of osteoblast-like cells on PLLA films with a biomimetic apatite or apatite/collagen composite coating.* Journal of Materials Science: Materials in Medicine, 2008. **19**(6): p. 2261-8.

37. Tajitsu, Y., et al., *Huge optical rotatory power of uniaxially oriented film of poly-L-lactic acid.* Journal Of Materials Science Letters, 1999. **18**: p. 1785– 1787.

38. Kurokawa, K., et al., *Surface properties and enzymatic degradation of end-capped poly(l-lactide).* Polymer Degradation and Stability, 2006. **91**(6): p. 1300-1310.

39. Bernardo, V., et al., *Cell behaviour in new poly(l-lactic acid) films with crystallinity gradients.* Materials Letters, 2012. **87**: p. 105-108.

40. Chang, H.M., et al., *Characterization and morphology analysis of degradable poly(l-lactide) film in in-vitro gastric juice incubation.* Applied Surface Science, 2012. **262**: p. 89-94.

41. Zhang, Y., et al., *Phase transition behavior of PLLA ultrathin film studied by grazing angle reflection absorption infrared spectroscopy.* Vibrational Spectroscopy, 2012. **63**: p. 338-341.

42. Mattioli, S., J.M. Kenny, and I. Armentano, *Plasma surface modification of porous PLLA films: Analysis of surface properties and in vitro hydrolytic degradation.* Journal of Applied Polymer Science, 2012. **125**(SUPPL. 2): p. E239-E247.

43. Rangari, D. and N. Vasanthan, *Study of strain-induced crystallization and enzymatic degradation of drawn poly(l-lactic acid) (PLLA) films.* Macromolecules, 2012. **45**(18): p. 7397-7403.

44. Hench, L.L. and J.R. Jones, *Biomaterials, artificial organs and tissue engineering*. Woodhead Publishing in Materials2005: Woodhead Publishing Limited. 286.

45. William D. Callister, J., *Materials Science and Engineering - An Introduction*. 7th ed2007: John Wiley & Sons, Inc.

46. Niinomi, M., *Recent Metallic Materials for Biomedical Applications.* Metallurgical And Materials Transactions, 2002. **33A**: p. 477-486.

47. Yang, K. and Y. Ren, *Nickel-free austenitic stainless steels for medical applications.* Science and Technology of Advanced Materials, 2010. **11**(1): p. 014105.

48. Lim, M.S., K.J. Smiley, and E.S. Gawalt, *Thermally driven stability of octadecylphosphonic acid thin films grown on SS316L.* Scanning, 2010. **32**(5): p. 304-11.

49. Ridwan, M.I.Z., et al., *Problem of Stress Shielding and Improvement to the Hip Implant Designs: A Review.* Journal of Medical Sciences, 2007. **7**(3): p. 460-467.

50. Lee, W.S., et al., *Dynamic Mechanical Response of Biomedical 316L Stainless Steel as Function of Strain Rate and Temperature.* Bioinorganic Chemistry and Applications, 2011. **2011**: p. 173782.

51. Niinomi, M., M. Nakai, and J. Hieda, *Development of new metallic alloys for biomedical applications.* Acta Biomaterialia, 2012. **8**(11): p. 3888-903.

52. Charles, L.F., et al., *Fabrication and mechanical properties of PLLA/PCL/HA composites via a biomimetic, dip coating, and hot compression procedure.* Journal of Materials Science: Materials in Medicine, 2010. **21**(6): p. 1845-54.

53. So, S., et al., *Correlation between metal allergy and treatment outcomes after ankle fracture fixation.* Journal of Orthopaedic Surgery, 2011. **19**(3): p. 309-13.

54. Niinomi, M., *Metallic biomaterials.* Journal of Artificial Organs, 2008. **11**(3): p. 105-10.

55. Silva, L.F.M., A. Ochsner, and R.D. Adams, *Handbook of Adhesion Technology*2011: Springer.

56. Rahme, R., et al., *New polymer/steel solution for automotive applications.* International Journal of Adhesion and Adhesives, 2011. **31**(7): p. 725-734.

57. Baldan, A., *Adhesively-bonded joints and repairs in metallic alloys, polymers and composite materials: Adhesives, adhesion theories and surface pretreatment.* Journal of Materials Science: Materials in Medicine 5, 2004. **39**: p. 1-49.

58. De Barros, S., et al., *Adhesion of Geopolymer Bonded Joints Considering Surface Treatments.* The Journal of Adhesion, 2012. **88**(4-6): p. 364-375.

59. Honkanen, M., et al., *Characterization of silane layers on modified stainless steel surfaces and related stainless steel–plastic hybrids.* Applied Surface Science, 2011. **257**(22): p. 9335-9346.

60. Hoikkanen, M., et al., *Effect of silane treatment parameters on the silane layer formation and bonding to thermoplastic urethane.* Progress in Organic Coatings, 2011. **72**(4): p. 716-723.

61. Yuan, W. and W.J.V. Ooij, *Characterization of Organofunctional Silane Films on Zinc Substrates.* Journal of Colloid and Interface Science, 1997. **185**: p. 197–209.

62. Lin, C.K. and C.C. Berndt, *Measurement and Analysis of Adhesion Strength for Thermally Sprayed Coatings.* Journal of Thermal Spray Technology, 1994. **3**(1): p. 75-104.

63. Delimi, A., et al., *Investigation of the corrosion behavior of carbon steel coated with fluoropolymer thin films.* Surface and Coatings Technology, 2011. **205**(16): p. 4011-4017.

64. Tüken, T., *Polypyrrole films on stainless steel.* Surface and Coatings Technology, 2006. **200**(16-17): p. 4713-4719.

65. Nazarov, A.P. and D. Thierry, *Scanning Kelvin probe study of metal/polymer interfaces.* Electrochimica Acta, 2004. **49**(17-18): p. 2955-2964.

66. Ryu, H., et al., *Polypyrrole film on 55% Al–Zn-coated steel for corrosion prevention.* Corrosion Science, 2012. **56**: p. 67-77.

67. González, M.B. and S.B. Saidman, *Electrodeposition of polypyrrole on 316L stainless steel for corrosion prevention.* Corrosion Science, 2011. **53**(1): p. 276-282.

68. Wang, Y. and D.O. Northwood, *An investigation into the nucleation and growth of an electropolymerized polypyrrole coating on a 316L stainless steel surface.* Thin Solid Films, 2008. **516**(21): p. 7427-7432.

69. Cieslik, M., et al., *Parylene coatings on stainless steel 316L surface for medical applications - Mechanical and protective properties.* Materials Science and Engineering C, 2012. **32**(1): p. 31-5.

70. Gallino, E., et al., *Plasma polymerized allylamine films deposited on 316L stainless steel for cardiovascular stent coatings.* Surface and Coatings Technology, 2010. **205**(7): p. 2461-2468.

71. Düdükcü, M. and F. Köleli, *Electrochemical synthesis of poly(5-nitroindole) on 316L-stainless steel in LiClO4-acetonitrile solution and its corrosion performance.* Progress in Organic Coatings, 2008. **62**(1): p. 1-4.

72. Kang, C.-K. and Y.-S. Lee, *Carbohydrate polymer grafting on stainless steel surface and its biocompatibility study.* Journal of Industrial and Engineering Chemistry, 2012. **18**(5): p. 1670-1675.

73. Gebhardt, F., et al., *Characterization of electrophoretic chitosan coatings on stainless steel.* Materials Letters, 2012. **66**(1): p. 302-304.

74. Wei, J., et al., *Stainless steel modified with poly(ethylene glycol) can prevent protein adsorption but not bacterial adhesion.* Colloids and Surfaces B: Biointerfaces, 2003. **32**(4): p. 275-291.

75. Ho, R.-M., et al., *Solvent-induced microdomain orientation in polystyrene-b-poly(l-lactide) diblock copolymer thin films for nanopatterning.* Polymer, 2005. **46**(22): p. 9362-9377.

76. Hall, D.B., P. Underhill, and J.M. Torkelson, *Spin Coating of Thin and Ultrathin Polymer Films.* Polymer Engineering and Science, 1998. **38**(12): p. 2039-2045.

77. Bornside, D.E., C.W. Macosko, and L.E. Scriven, *Spin coating: One-dimensional model.* Journal of Applied Physics, 1989. **66**(11): p. 5185.

78. Lizundia, E., S. Petisco, and J.-R. Sarasua, *Phase-structure and mechanical properties of isothermally melt-and cold-crystallized poly (L-lactide).* Journal of the Mechanical Behavior of Biomedical Materials, 2012.

79. Na, B., et al., *Evidence of sequential ordering during cold crystallization of poly (l-lactide).* Polymer, 2010. **51**(2): p. 563-567.

80. Yoshioka, T., et al., *Preparation of alginic acid layers on stainless-steel substrates for biomedical applications.* Biomaterials, 2003. **24**(17): p. 2889-2894.

81. Ford, J.L. and T.E. Mann, *Fast-Scan DSC and its role in pharmaceutical physical form characterisation and selection.* Advanced Drug Delivery Reviews, 2012. **64**(5): p. 422-30.

82. Awaja, F., et al., *Adhesion of polymers.* Progress in Polymer Science, 2009. **34**(9): p. 948-968.

83. Goddard, J.M. and J.H. Hotchkiss, *Polymer surface modification for the attachment of bioactive compounds.* Progress in Polymer Science, 2007. **32**(7): p. 698-725.

84. Bushroa, A.R., et al., *Approximation of crystallite size and microstrain via XRD line broadening analysis in TiSiN thin films.* Vacuum, 2012. **86**(8): p. 1107-1112.

85. Dadfar, M., et al., *Effect of TIG welding on corrosion behavior of 316L stainless steel.* Materials Letters, 2007. **61**(11-12): p. 2343-2346.

86. Arnoult, M., E. Dargent, and J.F. Mano, *Mobile amorphous phase fragility in semi-crystalline polymers: Comparison of PET and PLLA.* Polymer, 2007. **48**(4): p. 1012-1019.

87. Nejati, E., et al., *Needle-like nano hydroxyapatite/poly(l-lactide acid) composite scaffold for bone tissue engineering application.* Materials Science and Engineering: C, 2009. **29**(3): p. 942-949.

88. Cao, D., Z. Fu, and C. Li, *Heat and compression molded electrospun poly(l-lactide) membranes: Preparation and characterization.* Materials Science and Engineering: B, 2011. **176**(12): p. 900-905.

89. Touzin, M., et al., *Study on the stability of plasma-polymerized fluorocarbon ultra-thin coatings on stainless steel in water.* Surface and Coatings Technology, 2008. **202**(4884-4891).